Spectral characterisation of different glycerophospholipids using time-of-flight secondary ion mass spectrometry and matrix-assisted laser desorption/ ionisation time-of-flight mass spectrometry

DIPLOMARBEIT

ausgeführt zum Zwecke der Erlangung des akademischen Grades
eines **Diplom-Ingenieurs** im Rahmen des Studiums
der **Technischen Chemie**

unter der Leitung von
a.o. Prof. Dipl.-Ing. Dr.techn. Herbert **HUTTER**

eingereicht an der
Technischen Universität Wien
Fakultät für Technische Chemie
Institut für Chemische Technologien und Analytik

von
Roman Markus **HEFELE**
Matrikelnummer 0525063

Wien, Mai 2010

Spectral characterisation of different glycerophospholipids using time-of-flight secondary ion mass spectrometry (ToF-SIMS) and matrix-assisted laser desorption/ionisation time-of-flight mass spectrometry (MALDI-ToF)

Abstract: Glycerophospholipids have manifold functions in biochemistry. They are primary responsible for energy storage in organism and have important functions at the cellular signal transduction (e.g. in the sophisticated process of cell death). Therefore the distribution of the different glycerophospholipid species in a tissue section is important for the biological science. The determination of the lipid distribution with a high spatial resolution is a difficult task for the modern organic analytical chemistry. It results in two main requirements for the analytical technique: On the one hand the identification of the lipid has to be done very accurately and on the other hand the spatial resolution of the technique needs to be very high. The conventional used MALDI-ToF mass spectrometry technique provides an accurate identification of the lipid, but the low spatial resolution is a disadvantage. On the other hand the detection of large organic molecules can only be done with poly-atomic primary ions in the ToF-SIMS technique, because otherwise the energy of the incident primary ion is too high so that the fragmentation of large molecular ions is dominating. Through comparison between these two mass spectrometric analytical techniques it is demonstrated that even with the ToF-SIMS technique the identification of the glycerophospholipids with a high spatial resolution is possible. These analytical opportunity can be used for further imaging experiments with the ToF-SIMS so that in the future the lipid distribution of a tissue section can be visualised. Furthermore the peculiarities between the different primary ions and their influence in the fragmentation and ionisation processes of lipids in the ToF-SIMS technique are illustrated through comparison of the total ion yields and the different intensities of characteristic fragment ions. In addition to the analytical work a manual was developed which guides through the maintenance of the primary ion gun.

Keywords: ToF-SIMS • poly-atomic primary ions • MALDI-TOF mass spectrometrie • MS/MS experiments with CID and PSD • glycerophospholipids

Spektrale Identifizierung von verschiedenen Glycerophospholipiden mittels Flugzeit-Sekundärionenmassenspektrometrie (ToF-SIMS) und matrixunterstützte Laser-Desorption/Ionisation Flugzeitmassenspektrometrie (MALDI-ToF MS)

Kurzfassung: Glycerophospholipide haben in der Biologie eine sehr große Bedeutung, wobei die Substanzklasse der Lipide primär der Speicherung von Energie in Organismen dient. Darüber hinaus sind sie Strukturbestandteile in biologischen Membranen und haben essentielle Rollen in der Signaltransduktion (z.B. beim programmierten Zelltod). Daher ist es erforderlich die Verteilung von verschiedenen Glycerophospholipiden zum Beispiel in einem Gewebeschnitt zu kennen. Diese komplexe Anforderung an die moderne organische analytische Chemie setzt zwei Bedingungen voraus: So muss auf der einen Seite eine exakte Identifizierung der organischen Spezies erfolgen und zugleich sollte das Analysenverfahren eine hohe Ortsauflösung besitzen. Das dafür geeignete Verfahren der MALDI-ToF MS ermöglicht eine exakte Identifizierung, hat aber Nachteile in der Ortsauflösung. Durch polyatomare Bismut-Primärionen, ist es auch in der ToF-SIMS möglich, große organische Moleküle mit einer hohen Ortsauflösung zu detektieren. Es konnte durch Vergleich der beiden massenspektrometrischen Analysenverfahren gezeigt werden, dass ebenso mit der ToF-SIMS nicht nur eine Identifizierung der verschiedenen Lipide möglich ist. Durch die Verwendung von polyatomaren Primärionen ist es möglich den Ionisations- und Fragmentierungsprozess so zu beeinflussen, dass ebenso wie in der MALDI-ToF MS für ein Glycerophospholipid charakteristische Schlüsselfragmentionen gebildet werden. Diese Schlüsselfragmentionen können dann für weitere bildgebende Untersuchungen mittels der ToF-SIMS herangezogen werden. Um die Unterschiede zwischen den einzelnen Primärionen aufzuzeigen, wurden die einzelnen Intensitäten der verschiedenen Fragmentionen, sowie die totale Ionenausbeute eines Glycerophospholipids miteinander verglichen. Außerdem wird in der Arbeit auf die Wartung der Primärionenquelle des verwendeten ToF-SIMS-Gerätes eingegangen.

Schlagwörter: ToF-SIMS • Polyatomare Primärionen • MALDI-TOF Massenspektrometrie • MS/MS mittels CID und PSD • Glycerophospholipide

Acknowledgement

I want to thank ao. Prof. Herbert HUTTER for the possibility to perform my diploma thesis in his working group. He was at every time a sympathetic leader of his research group and beside the physical analytical strategies he held short history lections about the development of the modern time.
Of our research group I have to thank all other colleagues namely Dipl. Ing. Markus HOLZWEBER, Kurt PIPLITS, Dipl. Ing. Stefan PUCHNER, Dipl. Ing. Georg ZIEGLER and especially Dipl. Ing. Stefan KRIVEC and Dipl. Chem. Till FRÖMLING (working group of Prof. Jürgen FLEIG) for the instructions and the handling with the ToF-SIMS instrument.

The man which explained me that organic mass spectrometry of the well known glycerophospholipids is an exciting research topic was Mag. Dr. Ernst PITTENAUER. He was also responsible for the MALDI-ToF measurements of the glycerophospholipids and many scientific conversations concerning the biochemistry and pharmacy nature of these nice molecules.

I will also thank the non-scientific members of the institute Michael LUGER, Anna SATZINGER and Wolfgang TOMISCHKO for their help with the basic thinks beside the scientific work.

Finally I want to emphasis the patience and help of my parents during the last years of the study.

Contents

List of Figures

CHAPTER 1

Introduction

For many applications in the modern surface science imaging tools are required to understand the processes which are based on the local variation of the molecular concentration. Therefore the chemical mapping of organic and inorganic compounds on surfaces have a major relevancy for all research divisions (e.g. the influence of sodium in transistors) especially the distribution of biomarkers in tissue sections or cell cultures. There numerous different imaging techniques are available to detect and localise biological compounds with a tens of micrometer resolution, but most of these techniques need an amplification of the analytical signal for example with the help of fluorophore labelling [1].
The organic mass spectrometry is nowadays often used to solve the analytical problems of imaging various surfaces, without the disadvantages of overlapping signals for the UV [2] and Raman [3] spectroscopy. The sensitive fluorescent histochemical staining with Nile Red dye for phospholipids [2] is also no requirement for the mass spectrometry. For the imaging of tissue sections two main different techniques are commonly used which are based on the time-of-flight analyser: the matrix-assisted laser desorption/ionisation and the secondary ion mass spectrometry.

Glycerophospholipids which have manifold roles in biochemistry [4] and are considered as biomarkers for degenerative processes [5], cancer [6] and diabetes [7] are used in this diploma theses to demonstrate the difference between nanomolar sensitivity with MALDI-ToF versus nanometer resolution by ToF-SIMS [2].

Therefore a complete structural elucidation of three different phosphatidyl-choline lipids is done with MALDI-ToF. The observed results are used to interpret the ToF-SIMS spectra with respect to the characteristic fragment ions and their suitability for imaging of complex biological samples.

CHAPTER 2

Analytical strategy and methods

2.1 ToF-SIMS

2.1.1 Principles

Secondary ion mass spectrometry (abbreviation SIMS) generates and analyse the charged secondary ions which are induced by the bombardment of the sample surface with appropriate primary ions. Through interactions between the high energetic primary ions and the sample surface the emission and ionisation depending on the surface properties of the secondary ions takes place (see Figure 2.1). Therefore the investigation of the chemical composition related to the very top surface layers of the sample is possible. The first experiments for chemical surface analysis were in the 1960s [8, 9] based on the results of Herzog and Viehböck in the late 1940s [10].

The primary ions which are essentially for the process are generated by an ion source and subsequently guided through a sophisticated ion optic which produces a focused ion beam on the surface. Nowadays the liquid metal ion guns (LMIG) are used to generate the primary ions with a small spot size (depending on the detailed ion-optical set-up spot sizes between a few µm to 50 nm can be reached). The LMIG consist of a metal covered tungsten tip which forms under specific conditions (heating, extraction voltage) a so called taylor-cone. The desired primary ions are formed through field emission process at the apex of the taylor-come. The common metals which are used as LMIG materials are Au, Bi, Cs and In, whereas Au and Bi are used to form poly-atomic primary ions for the SIMS process [11, 12]. In our case the Bi-LMIG emitter produces Bi_n^+, n = 1 to 7, primary ions. The primary ions with the higher cluster size enhance the secondary ion yield and therefore they are of great interest for the investigation of organic structures like biological tissue sections.

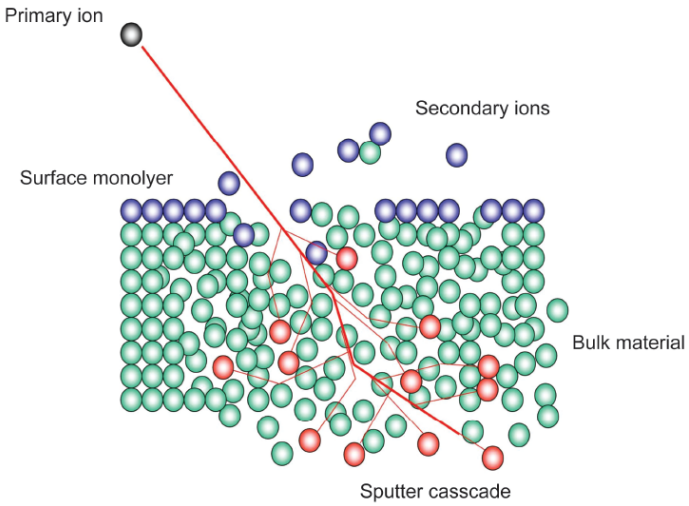

Figure 2.1: *Fundamental principles of the secondary ion formation (illustration from company-internal documents of Ion TOF, Germany)*

The formed secondary ions have to be separated and detected. Therefore different mechanisms are existing, but the majority of the spectrometer uses a time-of-flight or a sector field mass analyser. Both techniques separate the secondary ions on the mass to charge ratio m/z. For the separation depending on the detection principle different fundamental forces will be utilised. The sector field mass analyser applies different electrostatic and magnetic forces for ion separation. In the time-of-flight mass analyser the discrimination of the ions is based on the time which the ions need to pass a field free region. The assignment of the ion masses is done by the correlation of the detection event and the associated time o flight.

The ion detection is done with a micro channel plate connected to a charged coupled device (CCD) sensor. Through this technique a reliable detection ´of single ions is possible.

The ion current ion current was measured with a Faraday cup, where the current that belongs to the impact of the secondary ions is amplified and measured in a direct way [13].

2.1.2 Measurement settings

All ToF-SIMS measurements were carried out on a ToF-SIMS[5] instrument (Ion TOF, Germany) equipped with a Bi-LMIG as primary ion source. The emission current was set to 0.5 µA to obtain reasonable target currents for all desired primary ion species. The data were acquired in high current bunched mode with a mass resolution of approximately M/ΔM 5000. For every single measurement the primary ion dose density was adjusted to the in Table 1 specified values to ensure measurements within the static SIMS limit. The primary ion beam was scanned randomly over a total area of 300 x 300 µm with a 64 x 64 pixels raster. A charge compensation with the low energy electron flood gun was not required for the glycerophospholipids. The sample was measured on individual spots only in positive polarity at a cycle time of 135 µs to obtain all the desired molecular fragments. The mass calibration was done with the ions H (m/z 1.008), CH_3 (m/z 15.023), C_3H_7 (m/z 28.031), $C_5H_{12}N$ (m/z 86.097), $C_5H_{15}PNO_4$ (m/z 184.074) and $C_8H_{19}PNO_4$ (m/z 224.105).

	Bi_1^+	Bi_3^+	Bi_3^{++}	Bi_5^+
Ion current [pA]	0.570	0.275	0.230	0.020
Beam energy [kV]	25	25	25	25
Ion dose [cm^{-2}]	$1 \cdot 10^{10}$	$1 \cdot 10^{10}$	$1 \cdot 10^{10}$	$1 \cdot 10^{10}$
Raster [µm]	300	300	300	300
Pixels [-]	64 x 64	64 x 64	64 x 64	64 x 64

Figure 2.2: *Experimental parameters of the ToF-SIMS experiments*

2.2 MALDI-ToF

2.2.1 Principles

Through the invention of the matrix-assisted laser desorption/ionisation (MALDI) in the late 1980s based on the work of Hillenkamp and Karas [14] the chemically modification of phospholipids for the detection with the gas chromatography (GC) was not longer necessary. At the same time the physical properties of the time-of-flight mass analyser were optimised so that they had a better sensitivity and are able to detect large molecules.
The combination of MALDI with the time-of-flight mass analyser (ToF) was the beginning for the analytic of large organic molecules with a soft ionisation and the possibility to detect the intact protonated molecule ion. The advantage of MALDI-ToF in contrast to ESI is based on the type of the sample. So a liquid sample is need for the ESI technique while MALDI-ToF works only with solid samples.
The organic matrix is mixed with the sample and deposited on stainless steel targets. The generation of analyte ions is done by irradiating the sample surface with a pulsed UV or IR laser (usually N_2 (λ = 337 nm) or Nd/YAG (λ = 355 nm) lasers are used). Therefore the typically spot size of one single laser pulse is typically 50 µm. The laser radiation is absorbed by an appropriate organic matrix and the energy from the excited matrix is transformed to the organic analytes which are desorbed and ionised.
The generated ions are guided through a time-of-flight mass analyser and separated on the mass to charge ration which is based on the flight time through a field free path. Nowadays the ToF mass analyser has at the end of the linear flight path a reflectron. The reflectron has two different functions. First he reflects the incoming ions and increased therefore the flight path for the ions. On the other hand he works as an electrostatic mirror which separates the ions on their kinetic energy.
The combination of MALDI with the ToF mass analyser allows the simultaneous detection of numerous and various compounds (polymers,

peptides, metabolites, lipids, etc.) also in mixtures with an excellent sensitivity [2, 15].

For accurate structural elucidation post source decay (PSD) and collision induced decomposition (CID) MALDI-MS/MS experiments are necessary. Therefore an appropriate precursor ion is selected with the ion gate. In the case of the CID experiments the selected precursor ion has to pass a gas collision cell with helium as collision gas where the characteristic fragment ions of the precursor ion are formed. After the gas collision cell all ions have the same kinetic energy. Then the separation of the different masses with the same kinetic energy is done in the electrostatic field of the reflectron. Finally the fragment ions and the precursor ion is detected. In case of PSD MALDI-MS/MS the same process take place, but the gas collision cell is not filled with helium.

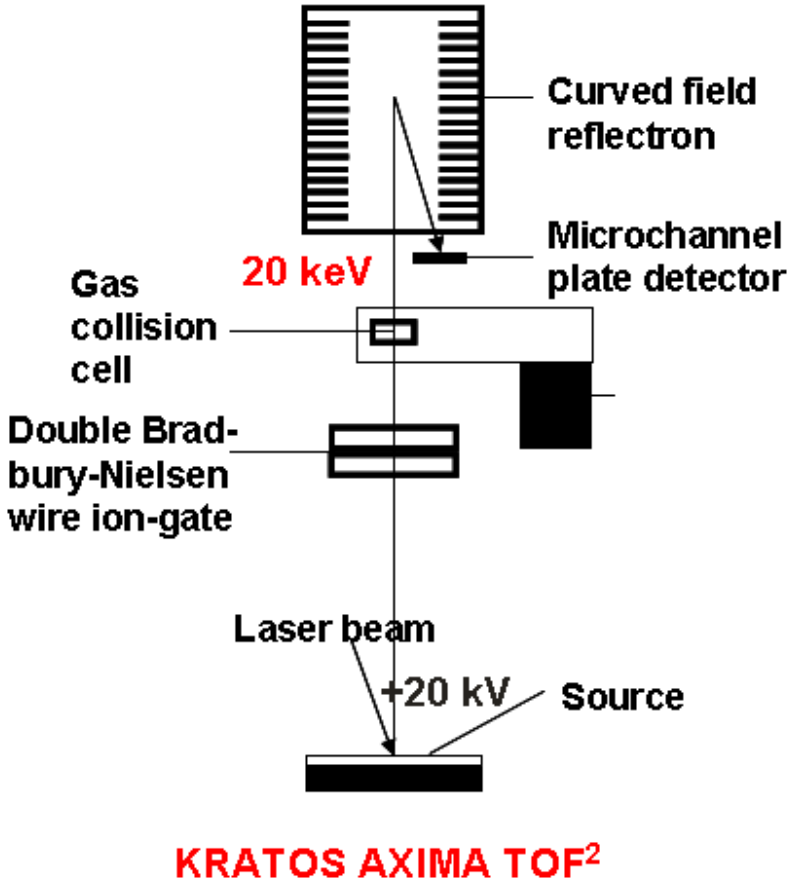

Figure 2.3: *MALDI-ToF instrument experimental instrumentation (illustration from E. Pittenauer, Vienna University of Technology, Austria)*

2.2.2 Measurement settings

All MALDI-ToF MS measurements were carried out on a AXIMA TOF^2 instrument (Kratos, UK) equipped with a pulsed N_2 laser at λ = 337 nm and an electrostatic mirror. The acceleration voltage was set at 20 kV. For the CID MS/MS experiments the signal-to-noise ratio was improved through use the average of 5000 single laser shots for one spectrum. In case of the PSD MS/MS experiments 1000 to 2000 single laser shots were used. The laser energy was for every spectrum individual optimised so that the signal intensity was maximised. Furthermore the laser beam was scanned over the whole matrix during the analysis of the sample and the pulsed extraction of the laser was set to an m/z of 800.

For the mass calibration of the spectra the ions of Na^+, K^+, $[M+H]^+$ of the matrix (THAP), $[M+Na]^+$ of the matrix, $[M+K]^+$ of the matrix and the $[M+H]^+$ and $[M+Na]^+$ of the phospholipid were used.
For the mass calibration of the PSD and CID MS/MS experiments the internal master file of the instrument which is based on the peptide P14R1 was used.

The structural elucidation of the different fragment ions was done with a sequentially approach starting with the protonated molecular ion peak. Then the functional groups of the precursor ion were eliminated systematically. So the structures of the characteristic fragment ions were determined and assigned with the suggested international nomenclature (see therefore literature [16]).

CHAPTER 3

Characterisation of Phospholipids

3.1 Introduction

The substance class of lipids is very simple in contrast to the rest of the comprehensive organic chemistry. Lipids are a condensation product of glycerol with three fatty acids in majority cases. There is even no commitment that these fatty acids have to be different. The simple molecule structure principle is almost the same, but for a comprehensive spectral characterisation with all possible combinations of fatty acid and alcohols still an infinite long time is needed. The circumstances, which reduce the possible number of combinations between fatty acids and glycerol, are that in nature and biological structures only sophisticated combinations of fatty acids with glycerol are present.

These combinations makes from a biochemistry point of view sense (e.g. lipogenesis: the fatty acid is built up from the two carbons of the acetyl-coenzyme A; therefore the fatty acid of the lipids has an even number of carbon atoms in the most cases of biological organism).

Therefore a categorisation of the lipids is based on the type of the polar head group, the individual molecular composition of the aliphatic chain and on the linking type between the aliphatic chain of the fatty acid and the glycerol (e.g. there can be an ester, ether or alkenyl as linking group) [17].

The biological structures of the lipids are not as simple as they will look at the first view. Nowadays we know that the condensation of two fatty acids and a phosphate group, which is an organic phosphoric acid ester between phosphoric acid and an organic alcohol, with the glycerol results in so called glycerophospholipids (see Fig. 3.1), which have important biological functions.

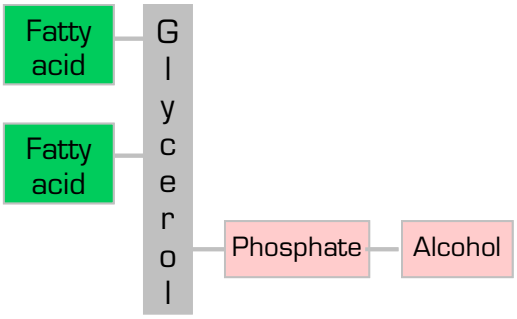

Figure 3.1: *Structure principle of glycerophospholipids*

The fatty acids in the phospholipid are responsible for the hydrophobic character and on the other hand the residual part of the molecule has hydrophilic properties. Nevertheless there are three different alcohols which are common in phospholipids of biological systems. The most common alcohol is glycerol, but other alcohols with three carbon atoms or the complex alcohol sphingosine (2-amino-4-octadecene-1,3-diol) are components of phospholipids. Therefore it is necessary to distinguish between phospholipids and glycerophospholipids, which specify that the main alcohol in the lipid chain is glycerol.

Hence the hydroxyl groups at the C-1 and C-2 of the glycerol are esterified with the carboxyl groups of the fatty acids and the C-3 hydroxyl groups is esterified with phosphoric acid.

Is at the phosphate function of the lipid the ester with an other alcohol is missing, then the lipid is called phosphatidate or diacylglycerol-3-phosphate, which occurs in low concentrations in membranes, but it is a key substance of the biosynthesis of other phosphoglycerols.

An important glycerophospholipid occurs when an ester is formed after condensation of a hydroxyl group of an alcohol with the phosphate group of the diacylglycerol-3-phosphate. Usually the alcohols are the amino acid serine, ethanolamine, choline, glycerol or inositol. The structures of these alcohols and the resulting glycerophospholipids are shown in Figure 3.2 and Figure 3.3.

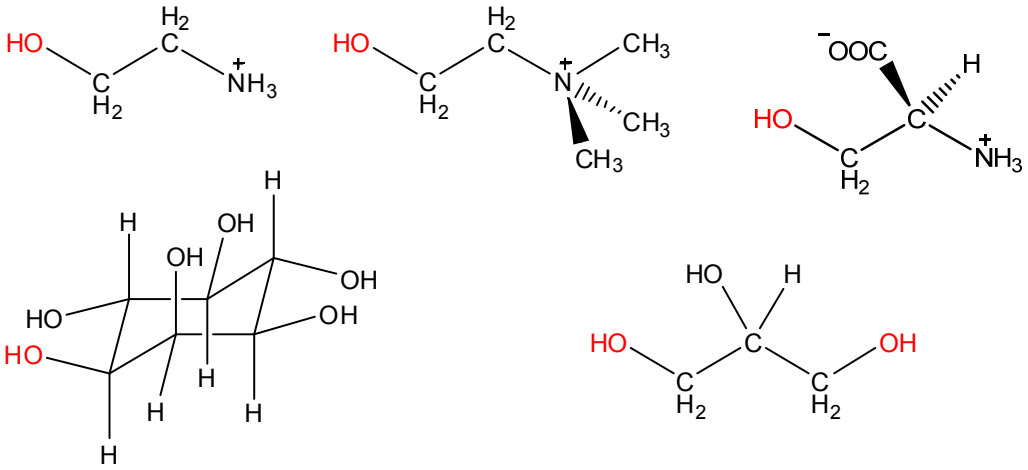

Figure 3.2: *The first line shows the structures of ethanolamine, choline, serine and the second the structures of inositol and glycerol.*

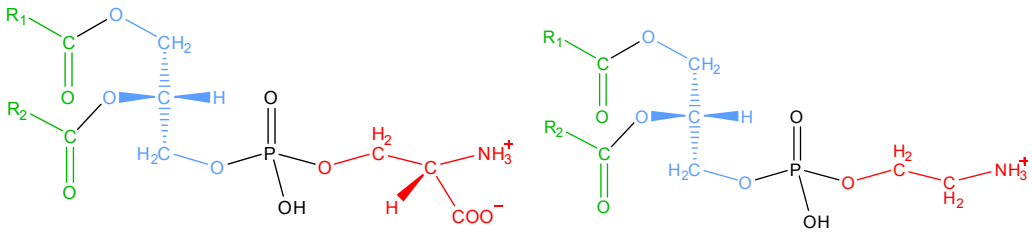

Phosphatidylserine

Phosphatidylethanolamine

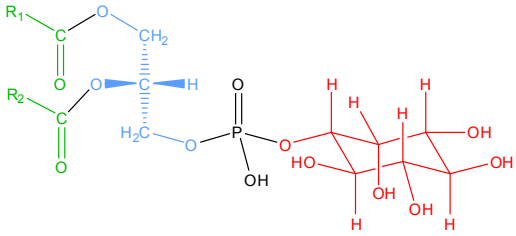

Phosphatidylinositol

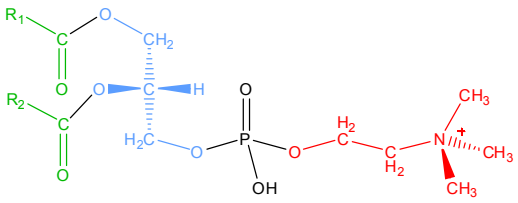

Phosphatidylcholine

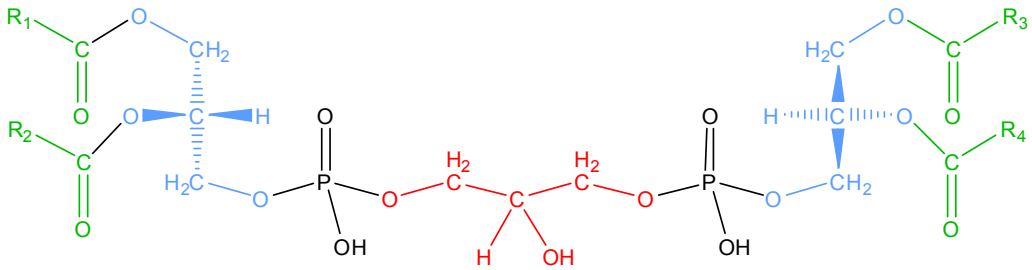

Diphosphatidylglycerol

Figure 3.3: *A selection of glycerophospholipids that are common in biological membranes.*

All different lipids, which are a part of biological membranes, have one common structure principle. They are amphiphilic molecules which have a hydrophilic and a hydrophobic region.
The space-filling model of a glycerophospholipid has an almost rectangular shape and both hydrophobic fatty acids are parallel to each other. The hydrophilic phosphorylcholine is oriented in the opposite direction of the fatty acids. This is shown in Figure 3.4.
As a consequence of the amphiphilic nature of the phospholipids, they establish a lipid bilayer which consists of two single lipid layers. In the lipid bilayer an interaction between the hydrophobic regions of the lipid takes place and so a hydrophobic internal space, which acts as a permeability barrier, is build up. The hydrophilic head groups of the lipids are in interaction with the enclosed aqueous medium (see Figure 3.5). In principle the phospholipids can establish also a micelle, which is a globular structure with the hydrophilic groups of the lipid on the outside of the sphere. But the preferred structure of phospholipids is the lipid bilayer, because both fatty acids are so space-consuming that they would not fit into the inner side of the sphere. (The micelle structure is preferred for salts of the fatty acids, e.g. sodium palmitate.)

The spontaneous formation of the lipid bilayers in water is a self-assembly process which is driven by the hydrophobic forces of the lipids. The consequence of this process is that the structure of the biological membranes is determined through the molecular properties of the lipids. In contrast to micelles, which are vigorous limited structures with a common diameter of about 20 nm, the lipid bilayer can reach macroscopic dimensions of some millimetres. That is the reason why phospholipids are important parts of biological membranes, because they can build up easily very large layers.
The reason why this form of biological membranes is so common and stable is that van der Waals attraction forces act between the large hydrophobic carbon skeleton of the fatty acids. So a close-packing of the different fatty acids happens. Finally a stabilisation of the membranes is done through electrostatic bonds and hydrogen bridges between the polar regions and the enclosed water molecules.

These each other amplifying non homopolar interactions results in cooperative structures which three features:

a) They have the attempt to maximise the occupied space.
b) They have the attempt to establish new bonds with itself, so that the borders with free carbon hydrogen chains are minimised, which leads to building of compartments.
c) They have the ability for self-repairing, because a hole in the lipid bilayer is immense energetically bad. [4]

Figure 3.4: *Space-filling model of a glycerophospholipid*

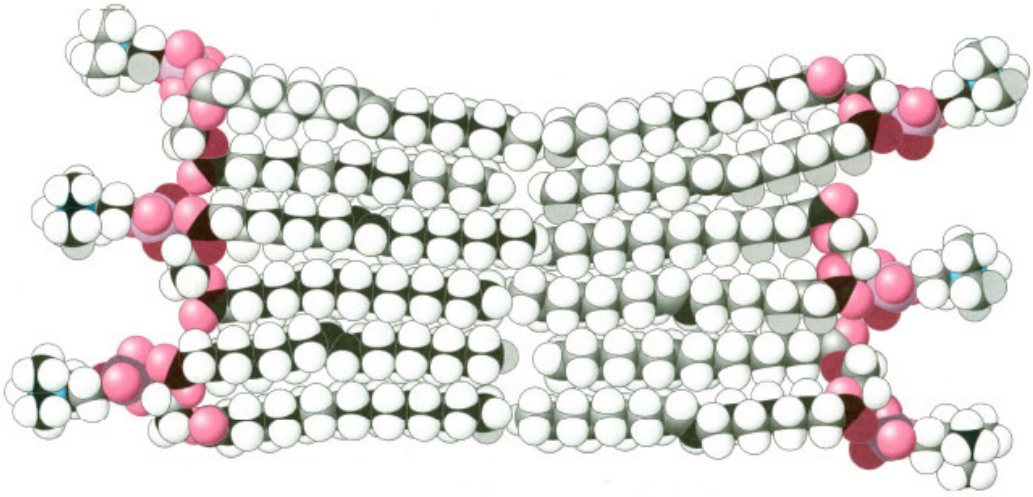

Figure 3.5: *Cross-section of the space-filling model of a phospholipid-bilayer membrane*

The diversity of lipids in general and glycerophospholipids in specific is extreme wide in cell metabolics and biochemistry. They have functions in energy production and storage, signal transduction and in the formation of the permeability barrier of cells an organells in form of a lipid bilayer [18].

Phospholipids or their derivates are also commonly used as biomarkers in geo- and microbiology, organic geochemistry, and microbial ecology [19].
The special interest of this work in phosphatidylcholine is a result of the significant effect which this class of glycerophospholipids in biological system have. Phosphatidylcholine is a content of all mammalian and some prokaryotic cells and has there critical roles in membrane structure and cellular signalling. Furthermore it is known that different cell types and tissues have a unique and stable profile of glycerophospholipid species. Another effect is that perturbation of phosphatidyl homeostasis in mammalian cells leads to cell death. This effect was verified through experimentally induced cell death systems which deciphered the cellular pathways for the physiological mechanism of programmed cell death.

The cell death is split into apoptosis and necrosis. The difference between these two cell death forms is that in case of the apoptosis the cellular membrane integrity is retained and in the other case the membranes are destroyed and the subcellular components are released to the immediate vicinity. In recent studies it is suggested that both forms, apoptosis and necrosis, are often inseparable events during cell death and they are sharing the same phosphatidylcholine mediators [20 – 23].

3.2 Spectral Characterisation of 1,2-Didocosanoyl-glycero-3-phosphocholine

3.2.1 Sample preparation

The glycerophospholipid namely 1,2-Didocosanoyl-glycero-3-phosphocholine (abbreviation PC 22:0-22:0) is commercially available (P-2342, Sigma-Aldrich, Austria). The lipid was stored at any time in a dark glass vial with Teflon septa and in a freezer at -18°C, except for preparing the sample solution.
For further analyses a lipid stock solution was prepared. Therefore 0.70 mg of the lipid were dissolved in 500 µL of a methanol-trichloromethane mixture (CH_3OH:$CHCl_3$ = 8:2). Therefore a commercially available methanol (34885, Sigma-Aldrich, Austria) and trichloromethane (288306, Sigma-Aldrich, Austria) were used. After that the dissolving process was completed by ultra-sonification for five minutes.

For the MALDI-ToF measurements[1] 2',4',6'-Trihydroxyacetophenone (91928, Sigma-Aldrich, Austria) as matrix was used. Again a stock solution of 10 mg 2',4',6'-Trihydroxyacetophenone (THAP) in 1000 µL methanol was prepared for all analyses and ultra-sonicated for 5 minutes to have a homogenous solution.
The MALDI-MS spots were prepared with the dried-droplet technique. Therefore 10 µL of the THAP stock solution and 10 µL of the lipid stock solution were homogenised in an Eppendorf tube. Then a MALDI target was cleaned by rinsing several times sequential with acetone (650501, Sigma-Aldrich, Austria) and 2-propanol (34965, Sigma-Aldrich, Austria).
After that 0.8 µL of the solution in the Eppendorf tube was transferred on a sample spot of a stainless steel target and the organic solvent was allowed to evaporate.

[1] in co-operation with E. Pittenauer, research group of (Bio)Polymer Analysis, Institute of Chemical Technologies and Analytics, Vienna University of Technology

This procedure was repeated several times so that at least five spots were available for the MALDI-TOF measurements. After preparation the target was introduced immediately into the vacuum chamber of the instrument.

Prior the preparation for the TOF-SIMS measurements the Si 111 wafer (Infineon, Austria) was carefully cleaned by ultra-sonification in a standard piranha etch solution (H_2O_2 : H_2SO_4 = 1 : 3; H_2O_2: 18312, Sigma-Aldrich, Austria; H_2SO_4: 84720, Sigma-Aldrich, Austria) and rinsed afterwards sequential with MilliQ-water (18.2 $M\Omega cm^{-1}$) and 2-propanol.
Then the silicon wafer was dried with high purity nitrogen. After that 5 µL of the lipid stock solution was placed with a pipette on the clean silicon wafer and the organic solvent was allowed to evaporate.
The deposition process was carried out in a laminar air flow box in order to prevent airborne particulate contamination. Finally the sample was mounted on the back mount sample holder and introduced immediately after preparation into the vacuum chamber of the instrument.

3.2.2 MALDI-ToF measurements results and discussion

The full MALDI-ToF spectrum (see Figure 3.6.) of 1,2-Didocosanoyl-glycero-3-phosphocholine (abbreviation: PC 22:0-22:0) shows three different precursor ions at m/z 902.8, m/z 925.8 and m/z 941.8. The first ion at m/z 902.8 is the protonated molecular ion of PC 22:0-22:0. The ions at m/z 925.8 and m/z 941.8 are the sodium and potassium adduct ions of the molecular ion.

The substance class of phosphocholine is proofed with the ions at m/z 58.1 and at m/z 86.1. These ions are from organic quaternary nitrogen molecule groups which are well-known markers for the choline group.
A direct identification of the whole phosphatidyl group is not possible, because the specific fragment ions at m/z 224.1, m/z 184 and m/z 166.1 are missing (see fragmentation scheme in Figure 3.9 and 3.10).

The very intense fragment ions at m/z 169.1, m/z 191.1 and m/z 207.0 are not from the phospholipid. They are the corresponding ions for the used MALDI-matrix of 2',4',6'-Trihydroxyacetophenone. Again the ion at m/z 169.1 is the protonated molecular ion peak. The other two peaks are the sodium and potassium adduct ions of the matrix.

The rest of the fragment ions of the lipid are not characteristic ions. They are built through the uncontrolled fragmentation processes and have no relation to systematic cleavage fragment ions from the precursor ions.

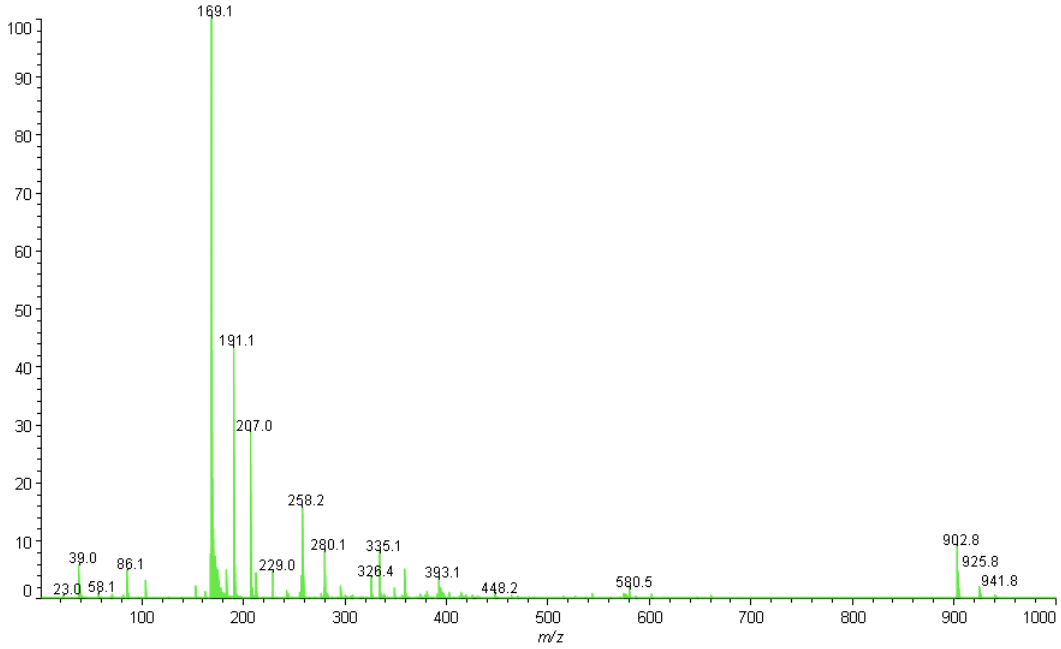

Figure 3.6: *Positive full MALDI-ToF spectrum of 1,2-Didocosanoyl-glycero-3-phosphocholine (PC 22:0-22:0)*

For characterisation of the glycerophospholipid a MALDI-ToF MS/MS collision induced decomposition (CID) experiment was done. Therefore the protonated molecular ion of the lipid was used as a precursor ion and the ion gate was set symmetrically at m/z 902.8 +/- 2.

This experiment allows now a systematic structural elucidation. The precursor ion at m/z 902.9 in the spectrum of Figure 3.7 was the molecular ion of the whole unfragmented lipid.

The following fragment ions with very low intensity in the range of m/z 650 to m/z 888 are characteristic for the cleavage of one carbon atom at the end of the fatty acid group. Through this process an olefin structure of the fatty acid is built and a fragment of m/z 16 is eliminated.

For the lipid the fragment ion at m/z 634.6 is a unique characteristic ion. This ion determines not only the type of phospholipid, but it is also unique for the fatty acids of the lipid.
The fragment ion indicated the partially loss of one fatty acid in a way that the carboxyl group remains on the fragment ion. Therefore the nomenclature labels this type of fragment ion with "A" with the remaining intact groups of the lipid in subscript. If the fatty acids of the lipid are not the same then two "A" fragment ions with different masses are formed.

When the cleavage eliminated the fatty acid in a way that only a hydroxyl group remains on the glycerophospholipid structure a "C + 18" fragment ion is built.
Additionally when the hydroxyl group is also lost then it is a so called "C" fragment ion. In the case of the "C" fragment ions only one fatty acid and the phosphocholine group are bond to the glycerol. The corresponding masses for the "C + 18" and "C" fragment ions are m/z 580.7 and m/z 562.7.

Generally the subscripts of the different fragment ions in Figure 3.7 determine the intact groups which a bond to the glycerol. All of the fragment ions which are part of the nomenclature are a marker for a class of phospholipids. The fragment ions A to C are unique for one single phospholipid.

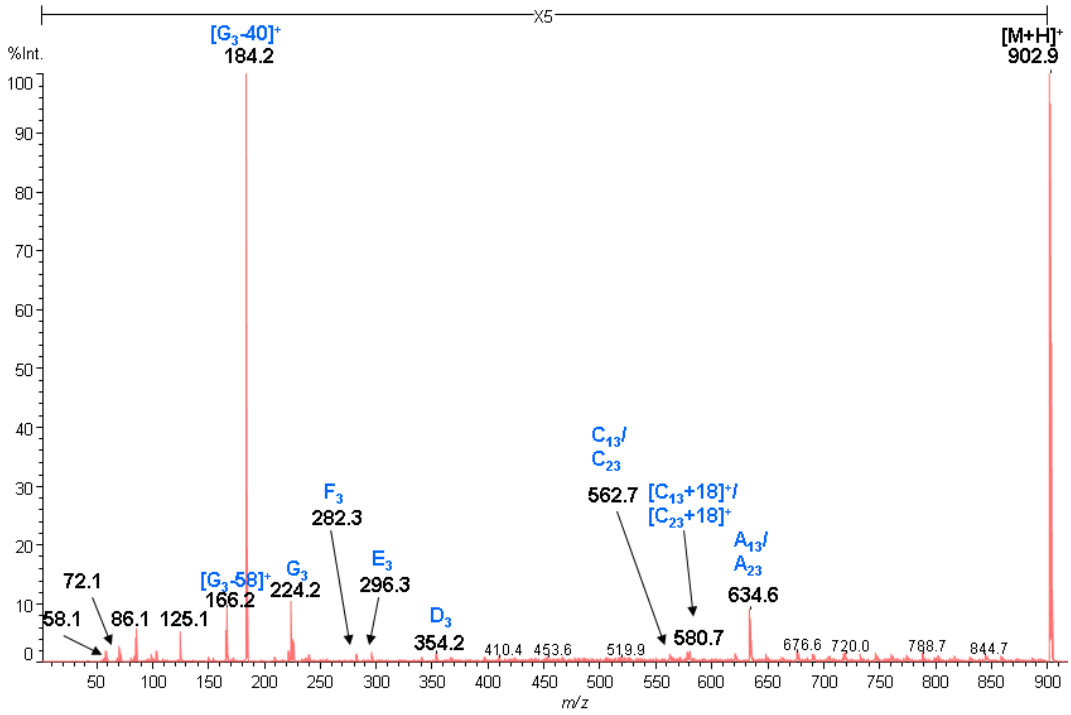

Figure 3.7: *Positive MALDI-CID spectrum of 1,2-Didocosanoyl-glycero-3-phosphocholine (PC 22:0-22:0) from the precursor ion at m/z 902.9*

The characteristic fragment ion at m/z 354.2 has partially lost both fatty acid chains so that the carboxyl groups are remaining on the molecule and therefore it is a "D" fragment ion.

Through rearrangements the fragment ions "E" and "F" at m/z 296.3 and 282.3 are built. At the "E" ion both fatty acids groups are eliminated and additionally a rearrangement reaction between the glycerol and the remaining carboxyl groups takes place and a tetrahydropyrane structure is formed. The same rearrangement reaction takes place to form the "F" fragment ion, but in contrast to the "E" ion a tetrahydrofuran heterocyclic structure is built up.

The "G" fragment ion at m/z 224.2 is the result of the complete loss of the fatty acids functions. The next fragment ions which occurs in the spectrum at m/z 184.2 and m/z 166.2 are specific losses of the complete glycerol group labelled with "G – 40" and additionally one oxygen atom of the phosphoric acid ester group which results in the "G - 58" fragment ion.

Both of the "G – 40" and "G - 58" fragment ion are characteristic fragment ions for the phosphocholine group.

In the lower mass range there are also some characteristic fragment ions which are not part of the used nomenclature. The protonated fragment ion at m/z 125.1 is a rearrangement of the phosphoric acid ester group. It determines the phospholipid class accurately, because of the low and odd-numbered molecular mass. (Remark: This ion is the only odd-numbered fragment ion of the spectrum.) The next two fragment ions at m/z 86.1 and m/z 72.1 are signalling molecules for the choline group which are built after complete cleavage of the phosphoric acid from the phosphocholine group.
The fragment ion at m/z 58.1 is a quaternary amino group which has lost the rest of the glycerophospholipid.

The spectral characterisation with the MALDI-ToF technique was completed with a MALDI-ToF MS/MS post source induced decay (PSD) experiment. For the PSD experiment the same instruments settings as for the CID experiment was used without the helium as collision gas.
The protonated molecular ion of the lipid was selected as a precursor ion and the ion gate was set symmetrically at m/z 902.8 +/- 2.

The PSD spectrum of the lipid PC 22:0-22:0 is shown in Figure 3.8. The mass at m/z 902.8 is the protonated molecular ion of the lipid which was the selected precursor ion. The fragment ion at m/z 580.6 has lost completely one fatty acid chain and is characteristic for the glycerophospholipid. The nomenclature of the fragment ion is "C + 18", because the hydroxyl group of the fatty acid is remaining.

For the characterisation of the phospholipid type the fragment ion of m/z 184.1 can be used. The two fatty acids groups and the glycerol group of the lipid are completely lost and the fragment ion is only the phosphoric acid ester of the choline.

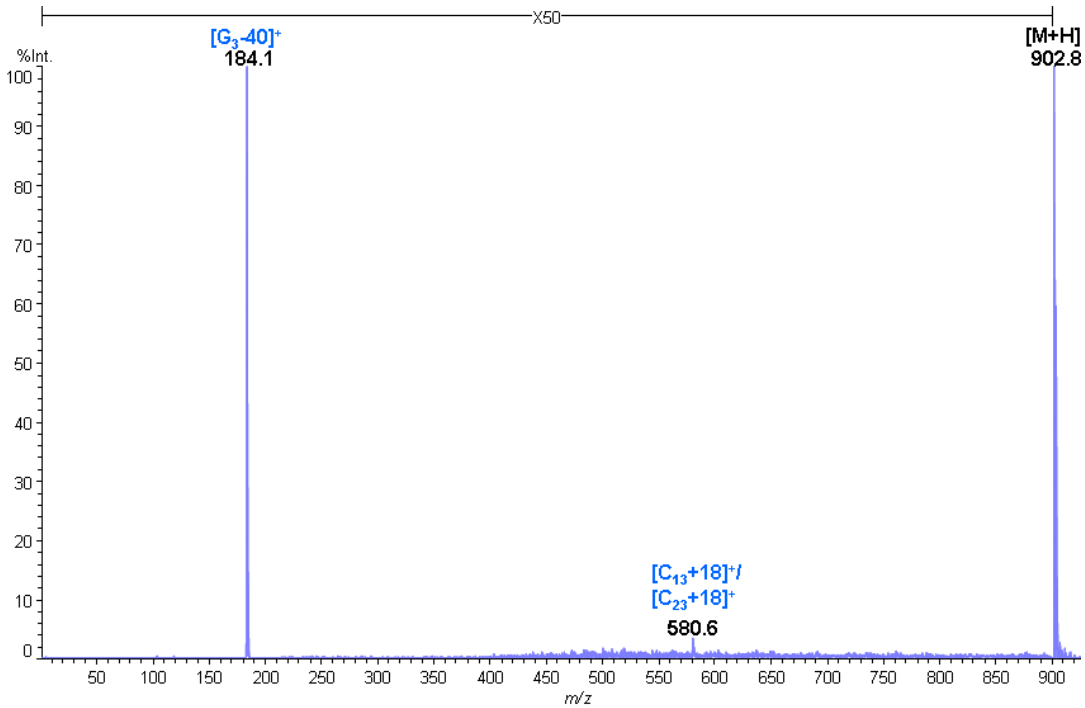

Figure 3.8: *Positive MALDI-PSD spectrum of 1,2-Didocosanoyl-glycero-3-phosphocholine (PC 22:0-22:0) from the precursor ion at m/z 902.9*

Further molecules are not detected in the PSD spectrum, because the PSD experiment generates only metastable ions. All other possible fragment ions are only formed when a collision gas atoms (in our case helium) is present.

Further molecules are not detected in the PSD spectrum, because the selected precursor ions have no collision with other atoms or ions through the flight time in the time-of-flight section in a PSD experiment. Therefore only metastable ions which are formed spontaneously from the precursor ion can be detected in this experiment.

The following Figures 3.9 and 3.10 describe the fragmentation scheme of the whole fragment ions which were detected through the CID experiment. The fragmentation scheme gives also an overview about the structural elucidation of the different fragment ions.

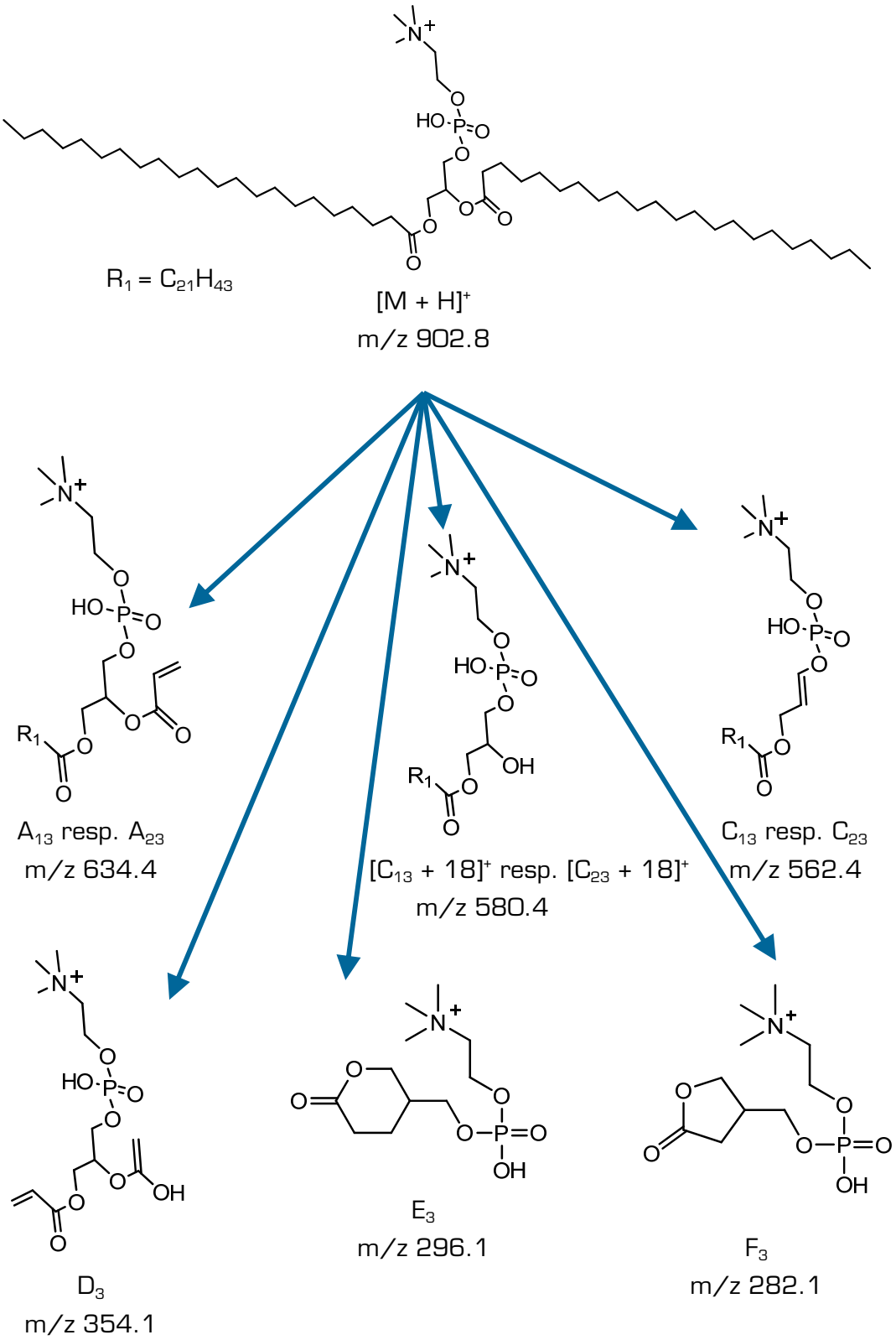

Figure 3.9: *Fragmentation scheme of PC 22:0-22:0 for the characteristic fragment ions "A" to "F" in the high mass range*

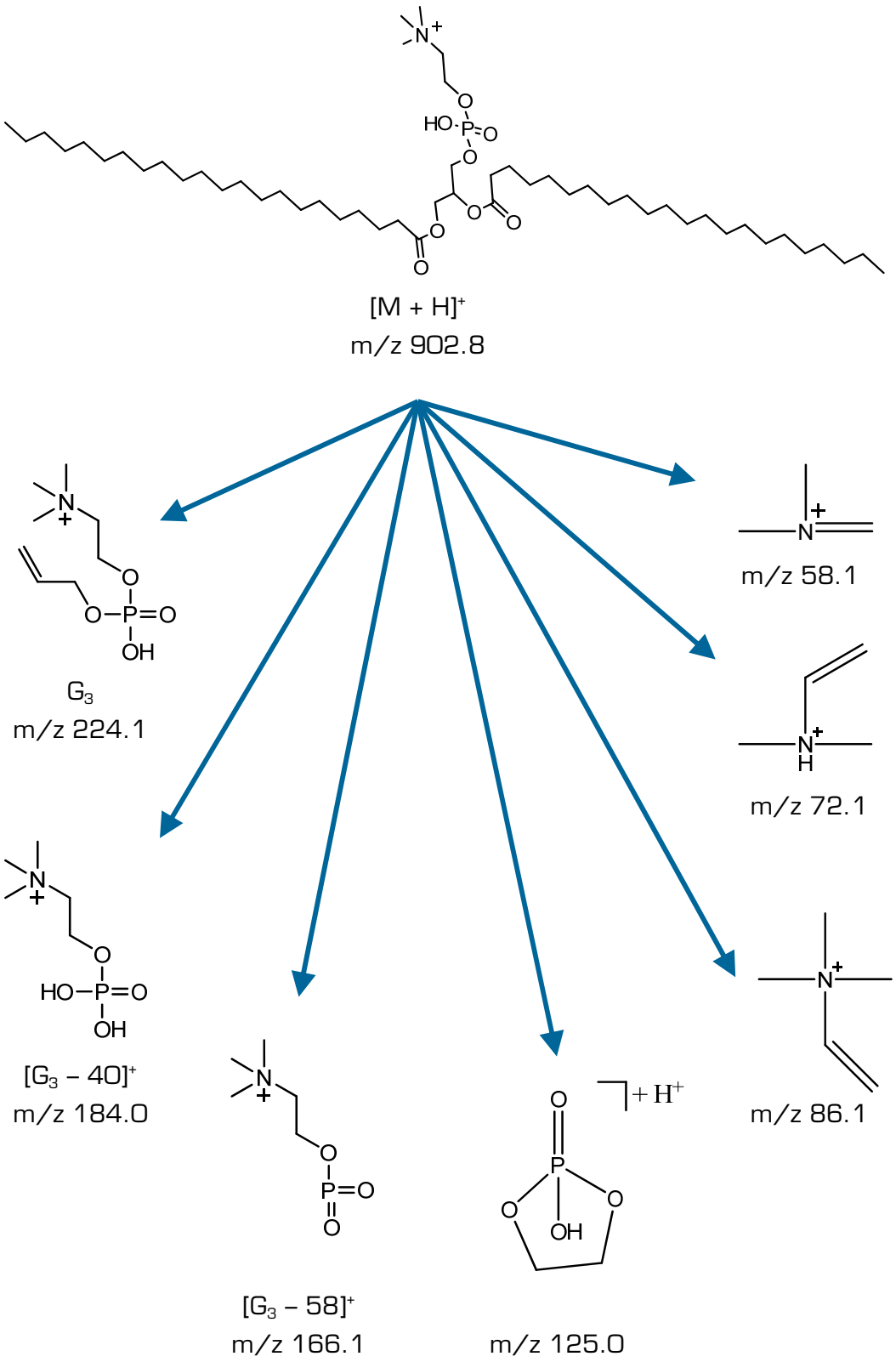

Figure 3.10: *Fragmentation scheme of PC 22:0-22:0 in the low mass range*

3.2.3 ToF-SIMS measurements results and discussion

The positive ToF-SIMS mass spectrum observed for PC 22:0-22:0, which is shown in Figure 3.12, reveals only a weak protonated molecule ion at m/z 902.4. The other obtained molecule ions with higher masses are not characteristic adduct ions in comparison to the MALDI-ToF spectrum (see Figure 3.6). Although the molecular ion is detected with the mass spectrometer, it can not be used for imaging experiments, because the intensity is therefore too low.
The characteristic fragment ion at m/z 634.5 has partially lost one fatty acid chain and is therefore declared as "A" ion from the MALDI-nomenclature. When the complete fatty acid chain is lost, then the "C" fragment ion at m/z 562.5 is formed. Both characteristic fragment ions can be used for identifying the whole glycerophospholipid, because one of the fatty acid functionality is remaining on the molecule. In the case of two different fatty acids two different "A" ions at different masses will be generated.

In the region of the low masses the "G" ions are formed. The fragment ions at m/z 224.2, m/z 184.1 and m/z 166.1 are characteristic for the phospholipid type. The fragment ion at m/z 224.2 has beside the phosphocholine group also a bonding to the main alcohol (in that case to glycerol).
According to the MALDI-CID spectrum also characteristic fragment ions for the phosphoric acid and amino group are generated. For the 5-membered phosphor heterocycle the ion at m/z 125.1 is formed. The ions at m/z 104.1, m/z 86.1, m/z 72.1 and m/z 58.1 contain a quaternary amino group and indicate the choline functionality of the lipid. The last three fragment ions are not shown in Figure 3.11, because the high intensity of these ions will discriminate the higher masses.

The additional molecular formula for the fragment ion at m/z 104.1 is shown in Figure 3.11.

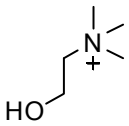

Figure 3.11: *Characteristic fragment ion at m/z 104.1 for PC 22:0-22:0 in the positive ToF-SIMS spectrum*

In contrast to the full MALDI-ToF and to the MALDI-PSD spectra (see Figure 3.6 and 3.8) it is demonstrated that with the help of the ToF-SIMS technique it is possible to have access to most of the characteristic fragment ions, so that an accurate determination of the different glycerophospholipids is possible.

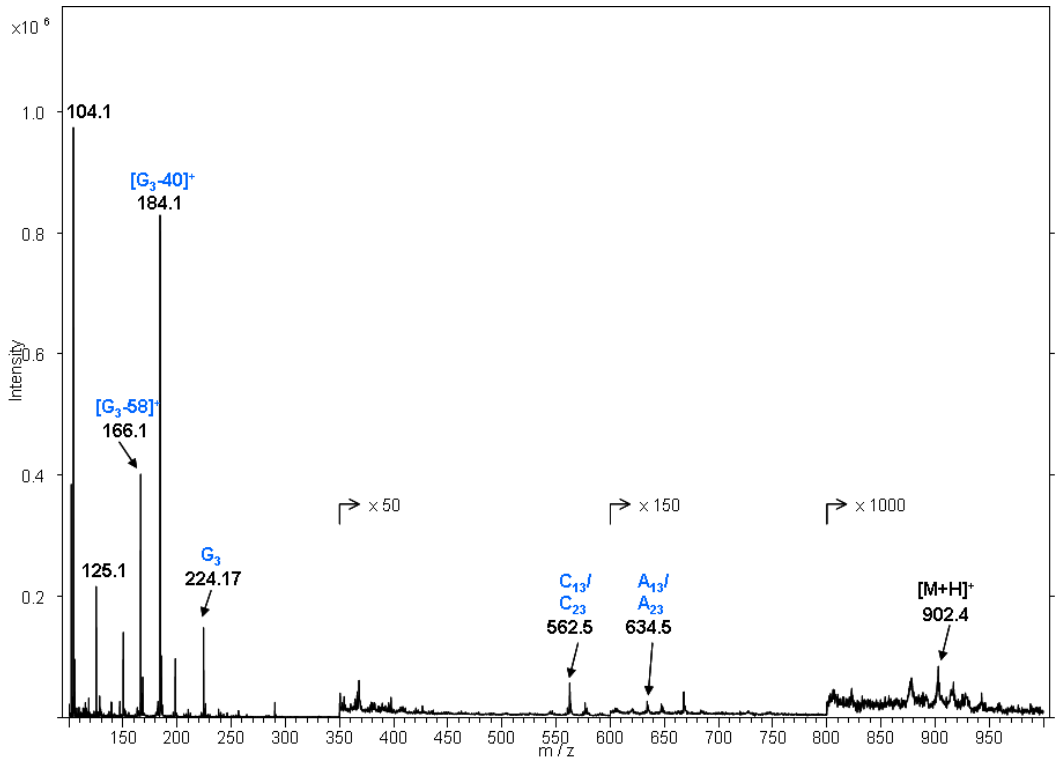

Figure 3.12: *Positive ToF-SIMS spectrum of PC 22:0-22:0 on a clean silicon wafer surface with Bi_3^{++} as incident primary ion with an acceleration voltage of 25kV*

The interaction of primary ions with the organic target molecules is depending on several processes which are not completely determined at all. In a first approximation an energy transfer of the kinetic energy of the primary ion to the organic target molecule is done. Therefore poly-atomic primary ions will cause different fragmentation and ionisation processes of the glycerophospholipid.

When mono-atomic primary ions are used then the large organic molecule is nearly complete fragmented. If poly-atomic primary ions interact with the organic target molecule then the fragmentation process can be decreased, because of the lower energy per single incident ion. This dependency is illustrated in Figure 3.13 for fragment ions in the lower mass range.

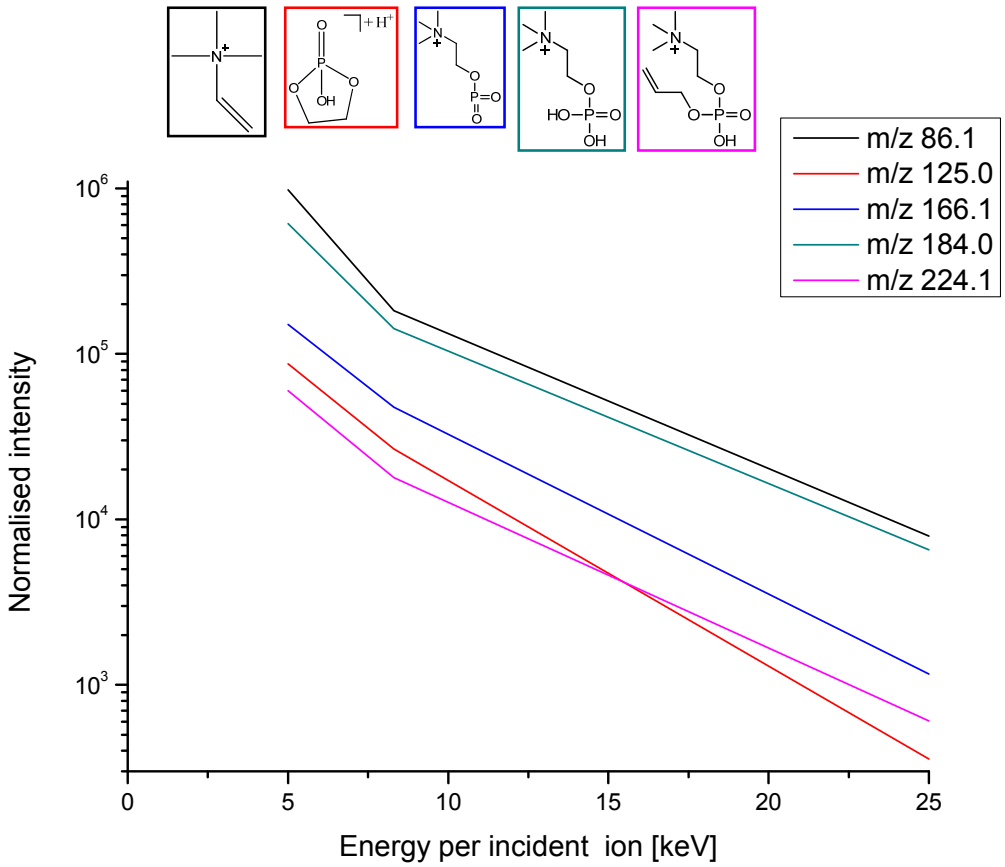

Figure 3.13: *Normalised intensities of different characteristic fragment ions in the low mass range as a function of the energy per incident atom for Bi_n^+, n= 1, 3, 5. Above the diagram the structures of the characteristic fragment ions are shown.*

A reduced energy per incident ion increases also the intensity of large fragment ions. Therefore the intensity of the "C" fragment ions can be increased by a factor of 100, when Bi_5^+ instead of Bi_1^+ is used. The protonated molecular ion and the "A" fragment ion can only be detected with poly-atomic primary ions; otherwise the high energy of the Bi_1^+ atoms will enable the fragmentation and dissociation of the precursor ion. In Figure 3.14 the influence of different primary ions on the intensity from the precursor and fragment ions is demonstrated.

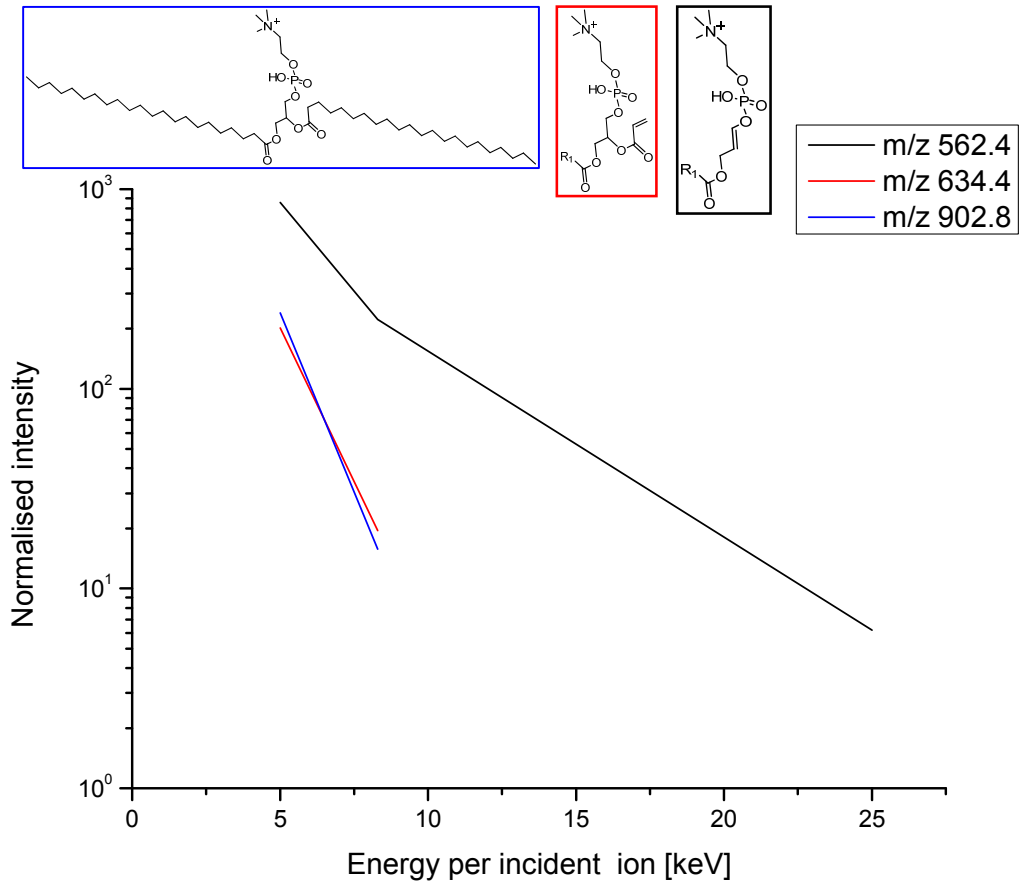

Figure 3.14: *Normalised intensities of different characteristic fragment ions in the high mass range as a function of the energy per incident atom for Bi_n^+, n= 1, 3, 5. Above the diagram the structures of the characteristic fragment ions are shown.*

With the ToF-SIMS instrument it is also possible to use double charged primary ions. Multiple charged primary ions do not influence the fragmentation and ionisation process in such a way that a significant enhancement of the fragment ions in the higher mass area is reached. For the most fragment ions it is no difference between the double and single charged primary ions. This is illustrated in Figure 3.15 for the PC 22:0-22:0. Only the intensity of the protonated molecule ion of the phospholipid can be increased when Bi_3^{++} instead of Bi_1^+ is used.

The reason why small primary ions are preferred for surface spectra than poly-atomic ions is that the measuring time for a specific primary ion dose will dramatically increase, because the higher bismuth primary ions have less ion currents and therefore more time is needed until the same ion dose of a mono-atomic primary ion is reached.

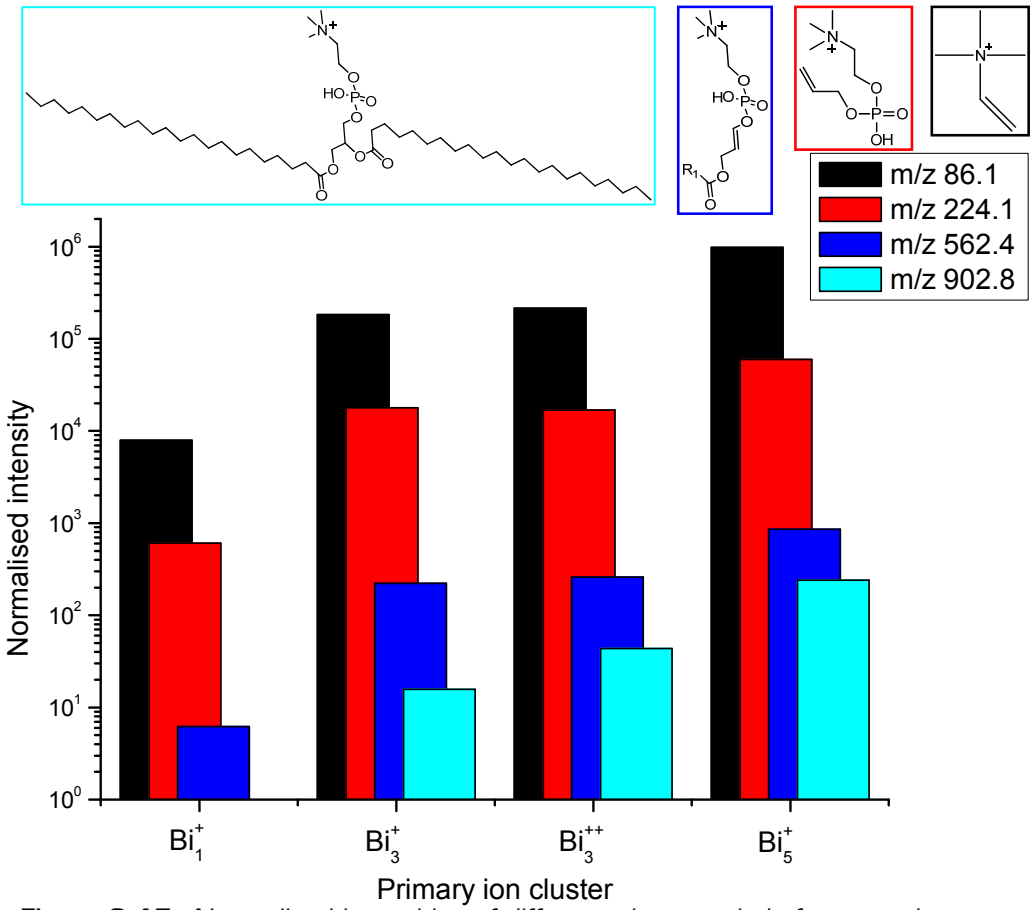

Figure 3.15: *Normalised intensities of different characteristic fragment ions as a function of the different primary ions (Bi_n^+, n= 1, 3, 5 and Bi_3^{++}). Above the diagram the structures of the characteristic fragment ions are shown.*

3.3 Spectral Characterisation of 1,2-Dipalmitoyl-glycero-3-phosphocholine

3.3.1 Sample preparation

The next glycerophospholipid for the spectral characterisation was 1,2-Dipalmitoyl-glycero-3-phosphocholine (abbreviation PC 16:0-16:0). This substance is commercially available (P-0763, Sigma-Aldrich, Austria). The glycerophospholipid was stored at any time in a dark glass vial with Teflon septa and in a freezer at -18°C, except for preparing the sample solution.
For further analyses a lipid stock solution was prepared. Therefore 0.50 mg of the lipid were dissolved in 500 µL of a methanol (CH_3OH). Therefore a commercially available methanol (34885, Sigma-Aldrich, Austria) was used. After that the dissolving process was completed by ultra-sonification for five minutes.

For the MALDI-ToF measurements[1] 2',4',6'-Trihydroxyacetophenone (91928, Sigma-Aldrich, Austria) as matrix was used. Again a stock solution of 10 mg 2',4',6'-Trihydroxyacetophenone (THAP) in 1000 µL methanol was prepared for all analyses and ultra-sonicated for 5 minutes to have a homogenous solution.
The MALDI-MS spots were prepared with the dried-droplet technique. Therefore 10 µL of the THAP stock solution and 10 µL of the lipid stock solution were homogenised in an Eppendorf tube. Then a MALDI target was cleaned by rinsing several times sequential with acetone (650501, Sigma-Aldrich, Austria) and 2-propanol (34965, Sigma-Aldrich, Austria).
After that 0.8 µL of the solution in the Eppendorf tube was transferred on a sample spot of a stainless steel target and the organic solvent was allowed to evaporate.

[1] in co-operation with E. Pittenauer, research group of (Bio)Polymer Analysis, Institute of Chemical Technologies and Analytics, Vienna University of Technology

This procedure was repeated several times so that at least five spots were available for the MALDI-TOF measurements. After preparation the target was introduced immediately into the vacuum chamber of the instrument.

Prior the preparation for the TOF-SIMS measurements the Si 111 wafer (Infineon, Austria) was carefully cleaned by ultra-sonification in a standard piranha etch solution (H_2O_2 : H_2SO_4 = 1 : 3; H_2O_2: 18312, Sigma-Aldrich, Austria; H_2SO_4: 84720, Sigma-Aldrich, Austria) and rinsed afterwards sequential with MilliQ-water (18.2 $M\Omega cm^{-1}$) and 2-propanol.
Then the silicon wafer was dried with high purity nitrogen. After that 5 µL of the lipid stock solution was placed with a pipette on the clean silicon wafer and the organic solvent was allowed to evaporate.
The deposition process was carried out in a laminar air flow box in order to prevent airborne particulate contamination. Finally the sample was mounted on the back mount sample holder and introduced immediately after preparation into the vacuum chamber of the instrument.

3.3.2 MALDI-ToF measurements results and discussion

The full MALDI-ToF spectrum (see Figure 3.16) of 1,2-Dipalmitoyl–glycero-3-phosphocholine (abbreviation: PC 16:0-16:0) indicate three different possible precursor ions at m/z 734.5, m/z 756.5 and m/z 773.5. The first ion at m/z 734.5 is the protonated molecular ion of PC 16:0-16:0. The ions at m/z 756.5 and m/z 773.5 are the sodium and potassium adduct ions of the molecular ion.

The substance class of phosphocholine is proofed with the fragment ion at m/z 86.1. This fragment ion consists of a quaternary amino group and is a well-known marker for the choline group.
A direct identification of the whole phosphatidyl group is not possible, because the specific fragment ions at m/z 224.1, m/z 184 and m/z 166.1 are missing (see fragmentation scheme in Figure 3.19 and 3.20).

The very intense fragment ions at m/z 169.1, m/z 191.1 and m/z 207.0 are not related to the phospholipid. They are the corresponding fragment ions for the used MALDI-matrix of 2',4',6'-Trihydroxyacetophenone. Again the ion at m/z 169.1 is the protonated molecular ion peak. The other two peaks are the sodium and potassium adduct ions of the matrix.

The rest of the fragment ions of the lipid are not characteristic cleavage fragments from one of the precursor ions, because they were built through uncontrolled fragmentation processes.

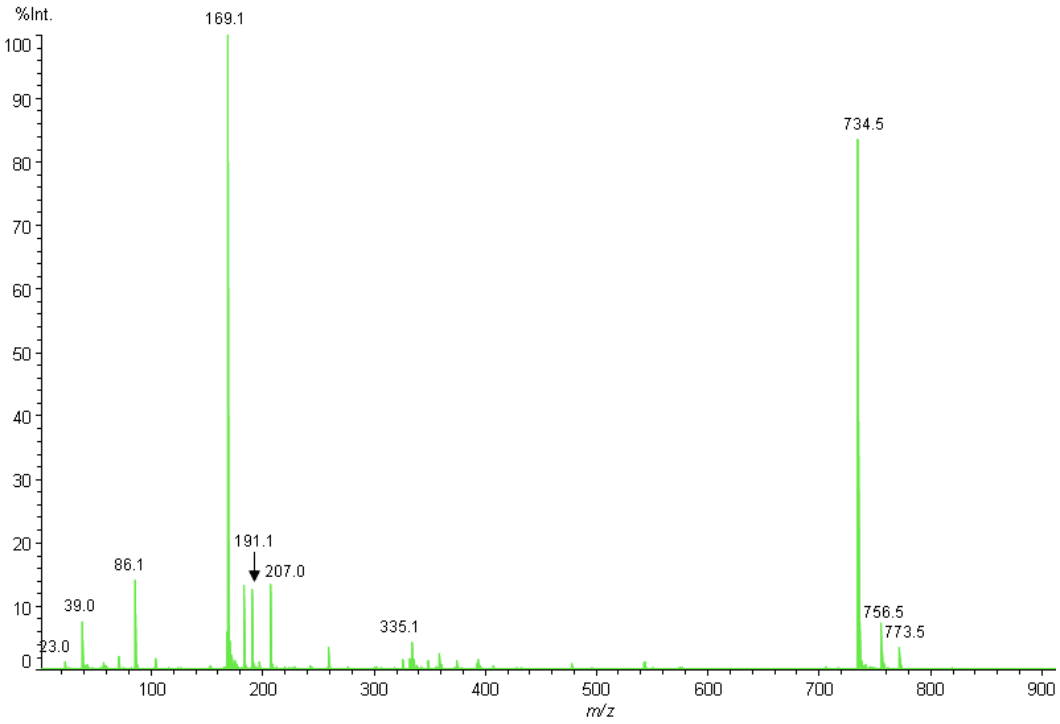

Figure 3.16: *Positive full MALDI-ToF spectrum of 1,2-Dipalmitoyl-glycero-3-phosphocholine (PC 16:0-16:0)*

For characterisation of the glycerophospholipid a MALDI-ToF MS/MS collision induced decomposition (CID) experiment was done. Therefore the protonated molecular ion of the lipid was used as a precursor ion and the ion gate was set symmetrically at m/z 734.5 +/- 2.

Based on these results a systematic structural elucidation from the precursor ion at m/z 734.5 is possible. For the spectrum see Figure 3.17.

The fragment ions in the range of m/z 560 to m/z 700 are characteristic for the cleavage of one carbon atom at the end of the fatty acid group. In the process an olefin structure of the fatty acid is formed and a fragment ion of m/z 16 is eliminated.

For the lipid the "A" fragment ion at m/z 550.3 is a unique characteristic fragment ion. This ion determines not only the type of phospholipid, but it is also unique for the fatty acids of the lipid.
The fragment ion indicated the partially loss of one fatty acid in a way that the carboxyl group remains on the fragment ion. If the lipid has different fatty acids two "A" fragment ions at different masses will be formed.

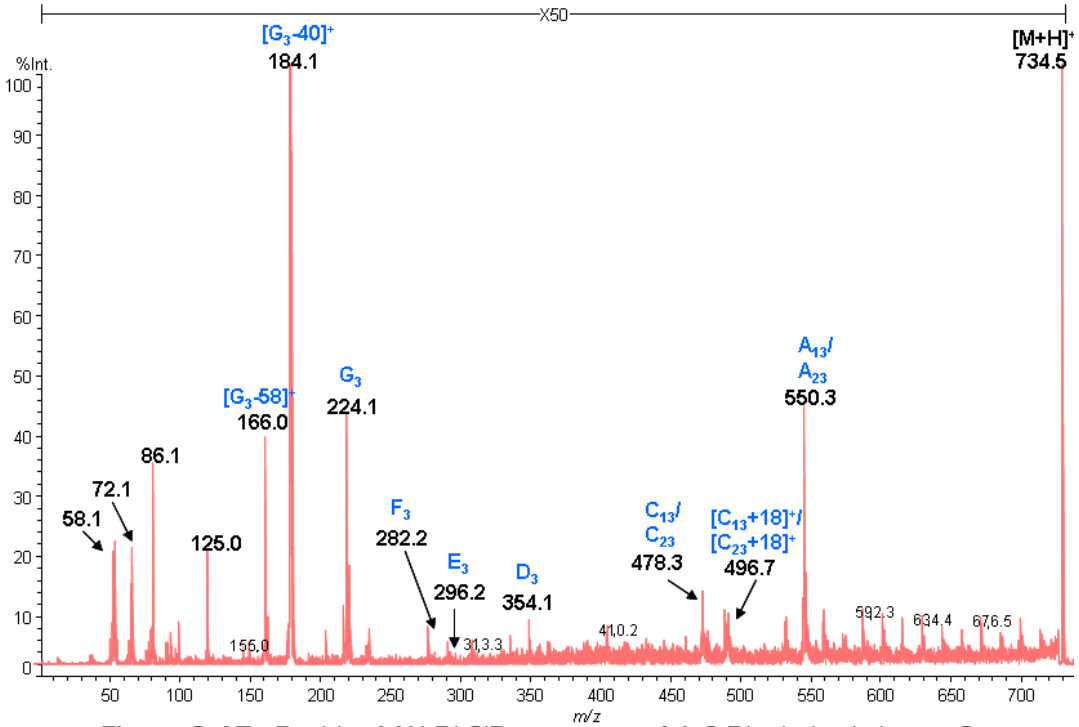

Figure 3.17: *Positive MALDI-CID spectrum of 1,2-Dipalmitoyl-glycero-3-phosphocholine (PC 16:0-16:0) from the precursor ion at m/z 734.5*

For the PC 16:0-16:0 the "C + 18" and "C" fragment ions are at m/z 496.7 and m/z 478.3. If the fatty acid is eliminated and only the hydroxyl group remains on the glycerophospholipid structure the "C + 18" fragment ion is formed. If the fatty acid is completely eliminated from the lipid then the resulting ion is a so called "C" fragment ion.

The characteristic "D" fragment ion at m/z 354.1 has a partially cleavage in both fatty acid chains so that the carboxyl groups are remaining on the molecule.

Through rearrangement reactions the fragment ions "E" and "F" at m/z 296.3 and 282.3 are formed. At the "E" ion both fatty acids chains are eliminated and additionally a rearrangement reaction between the glycerol and the remaining carboxyl groups takes place. As a consequence a tetrahydropyrane structure is formed. The same rearrangement reaction takes place to form the "F" fragment ion, but in contrast to the "E" ion a tetrahydrofuran heterocyclic structure results.

The "G" fragment ion at m/z 224.1 has a complete loss of the fatty acids functions and determines only the type of phospholipid, because it consists of the glycerol and phosphocholine functionalities. The next fragment ions which occur in the spectrum at m/z 184.1 and m/z 166.0 are specific losses of the complete glycerol group labelled with "G – 40" and additionally one oxygen atom of the phosphoric acid ester group which results in the "G - 58" fragment ion.

In the lower mass range there are also some characteristic fragment ions which are not part of the used nomenclature. The protonated fragment ion at m/z 125.1 is a rearrangement of the phosphoric acid ester group. It determines the phospholipid class accurately, because of the low and odd-numbered molecular mass. (Remark: This ion is the only odd-numbered fragment ion of the spectrum.) The next two fragment ions at m/z 86.1 and m/z 72.1 are signalling molecules for the choline group which are built after complete cleavage of the phosphoric acid from the phosphocholine group.

The fragment ion at m/z 58.1 is a quaternary amino group which has lost the rest of the glycerophospholipid.

The spectral characterisation with the MALDI-ToF technique was completed with a MALDI-ToF MS/MS post source induced decay (PSD) experiment. For the PSD experiment the same instruments settings as for the CID experiment was used without the helium as collision gas.
The protonated molecular ion of the lipid was selected as a precursor ion and the ion gate was set symmetrically at m/z 734.6 +/- 2.

The PSD spectrum of the lipid PC 16:0-16:0 is shown in Figure 3.18. The mass at m/z 734.6 is the protonated molecular ion of the glycerophospholipid. The fragment ion at m/z 496.7 has lost completely one fatty acid chain and is characteristic for the glycerophospholipid. The nomenclature of the fragment ion is "C + 18", because the hydroxyl group of the fatty acid is remaining.

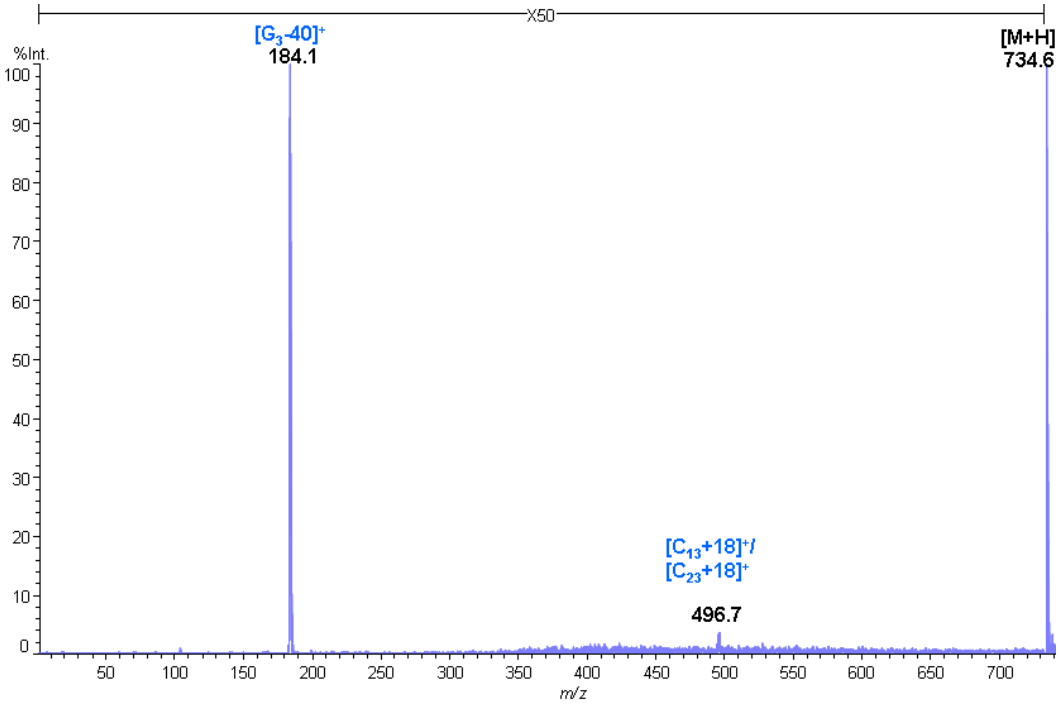

Figure 3.18: *Positive MALDI-PSD spectrum of 1,2-Dipalmitoyl-glycero-3-phosphocholine (PC 16:0-16:0) from the precursor ion at m/z 734.6*

For the characterisation of the phospholipid type the fragment ion of m/z 184.1 can be used. The two fatty acids groups and the glycerol group of the lipid are completely lost and the fragment ion is only the phosphoric acid ester of the choline.

Further molecules are not detected in the PSD spectrum, because the selected precursor ions have no collision with other atoms or ions through the flight time in the time-of-flight section of a PSD experiment. Therefore only metastable ions which are formed spontaneously from the precursor ion can be detected in this experiment.

The following Figures 3.19 and 3.20 describe the fragmentation scheme of the whole fragment ions which were detected through the CID experiment. The fragmentation scheme gives also an overview about the structural elucidation of the different fragment ions.

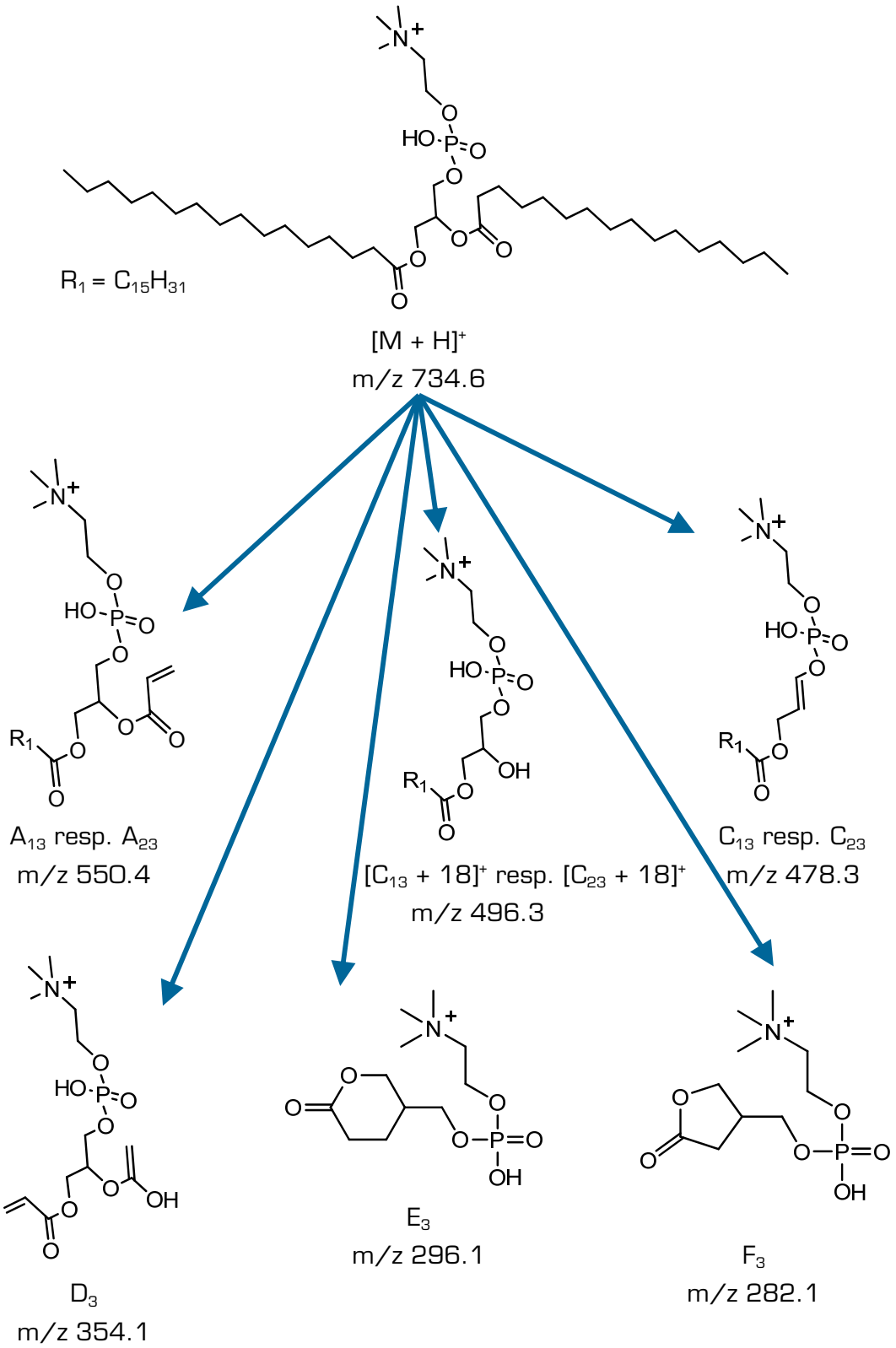

Figure 3.19: *Fragmentation scheme of PC 16:0-16:0 for the characteristic fragment ions "A" to "F" in the high mass range*

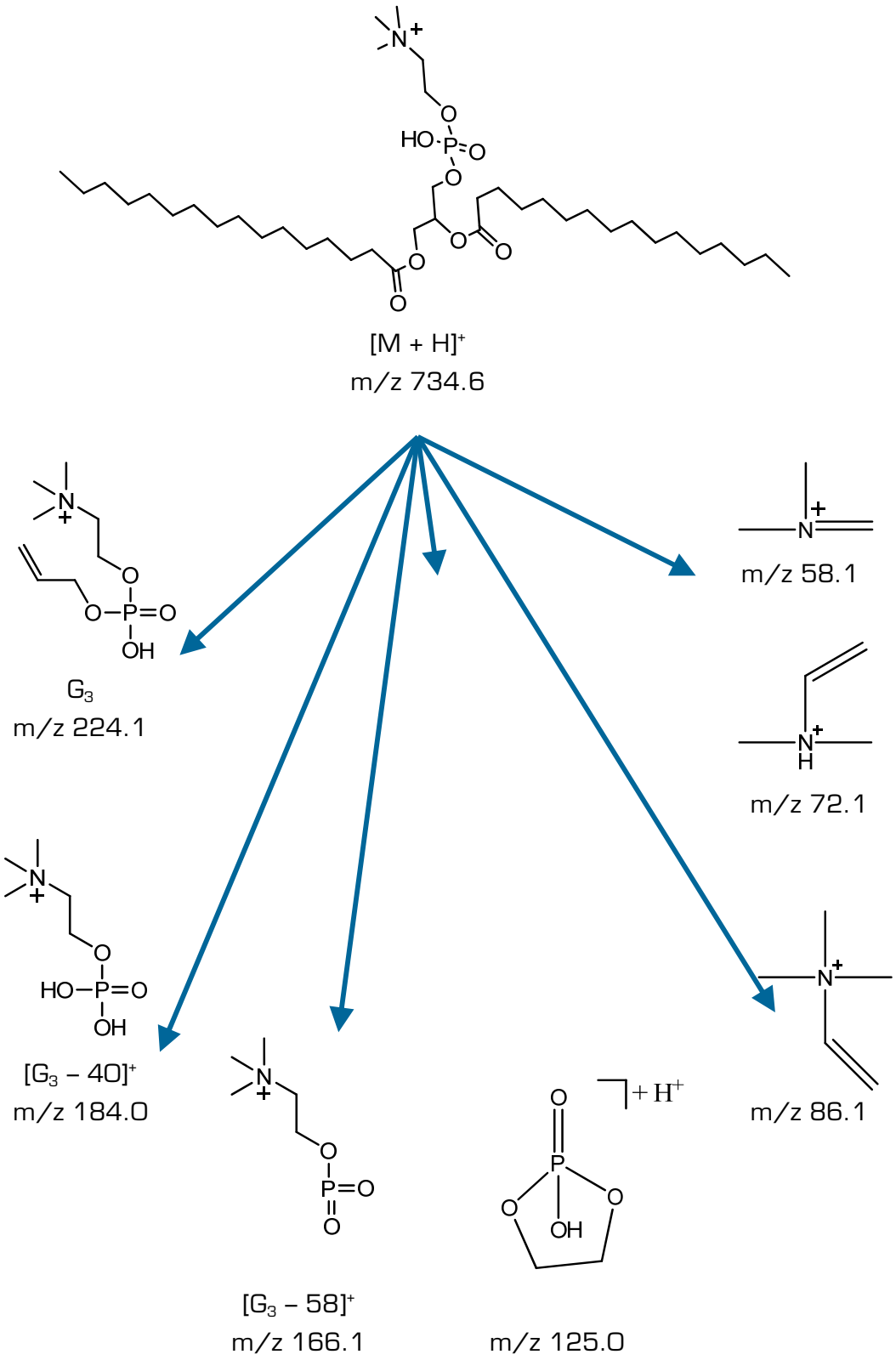

Figure 3.20: *Fragmentation scheme of PC 16:0-16:0 in the low mass range*

3.3.3 ToF-SIMS measurements results and discussion

The positive ToF-SIMS mass spectrum observed for PC 16:0-16:0, which is shown in Figure 3.21, reveals only a weak protonated molecule ion at m/z 734.5. The broad weak peak at m/z 757.5 indicates uncertainly the sodium adduct ion of the molecule ion. Therefore other obtained molecule ions with higher masses then m/z 734.5 are not characteristic adduct ions in comparison to the MALDI-ToF spectrum (see Figure 3.16). Although the molecular ion is detected with the mass spectrometer, it can not be used for characterisation or imaging experiments of the lipid, because the intensity is therefore too low.
The characteristic fragment ion at m/z 550.5 has partially lost one fatty acid chain and is therefore declared as "A" ion from the MALDI-nomenclature. When the complete fatty acid chain is lost, then the "C" fragment ion at m/z 478.4 is formed. Both characteristic fragment ions can be used for identifying the whole glycerophospholipid, because one of the fatty acid functionality is remaining on the molecule. In the case of two different fatty acids two different "A" ions at different masses will be generated.

In the region of the low masses the "G" ions are formed. The fragment ions at m/z 224.1, m/z 184.2 and m/z 166.1 are characteristic for the phospholipid type. The fragment ion at m/z 224.2 has beside the phosphocholine group also a bonding to the main alcohol (in that case to glycerol).

According to the MALDI-CID spectrum also characteristic fragment ions for the phosphoric acid and amino group are generated. For the 5-membered phosphor heterocycle the ion at m/z 125.1 is formed. The ions at m/z 104.1, m/z 86.1, m/z 72.1 and m/z 58.1 contain a quaternary amino group and indicate the choline functionality of the lipid. The last fragment ion are not shown in Figure 3.21, because the high intensity of this ion will discriminate the higher masses.

For the fragmentation scheme see Figure 3.19 and 3.20. The additional molecular formula for the fragment ion at m/z 104.1 is shown in Figure 3.11.

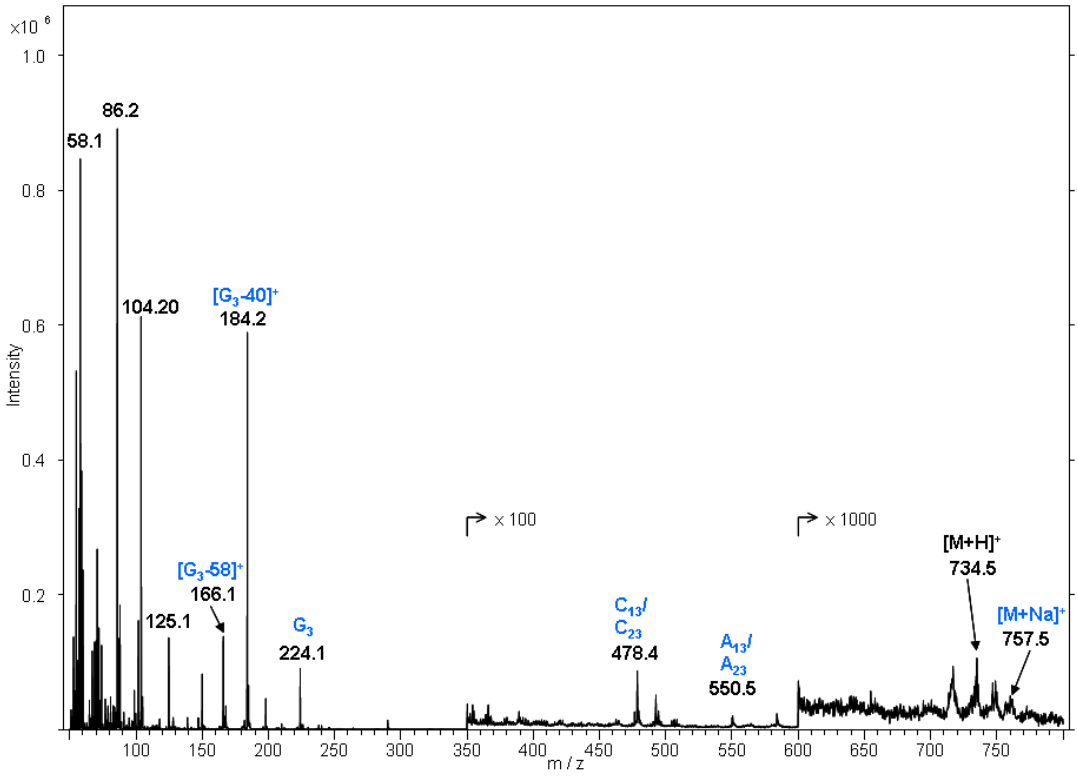

Figure 3.21: *Positive ToF-SIMS spectrum of PC 16:0-16:0 on a clean silicon wafer surface with Bi_3^{++} as incident primary ion with an acceleration voltage of 25kV*

In contrast to the full MALDI-ToF and to the MALDI-PSD spectra (see Figure 3.16 and 3.18) it is demonstrated that with the help of the ToF-SIMS technique it is possible to have access to most of the characteristic fragment ions, so that an accurate determination of the different glycerophospholipids is possible.

For the PC 16:0-16:0 the dependency between the type of the primary ion and the intensity of the characteristic fragment ion is illustrated in Figure 3.22. The interaction of primary ions with the organic target molecules is depending on several processes which are not completely determined at all. In a first approximation an energy transfer of the kinetic energy of the primary ion to the organic target molecule is done. Therefore poly-atomic primary ions will cause different fragmentation and ionisation processes of the glycerophospholipid.

When mono-atomic primary ions are used then the large organic molecule is nearly complete fragmented. If poly-atomic primary ions interact with the organic target molecule then the fragmentation process can be decreased, because of the lower energy per single incident ion. The Figure 3.22 shows that incident ions with reduced energies increase the intensity of lager characteristic fragment ions.

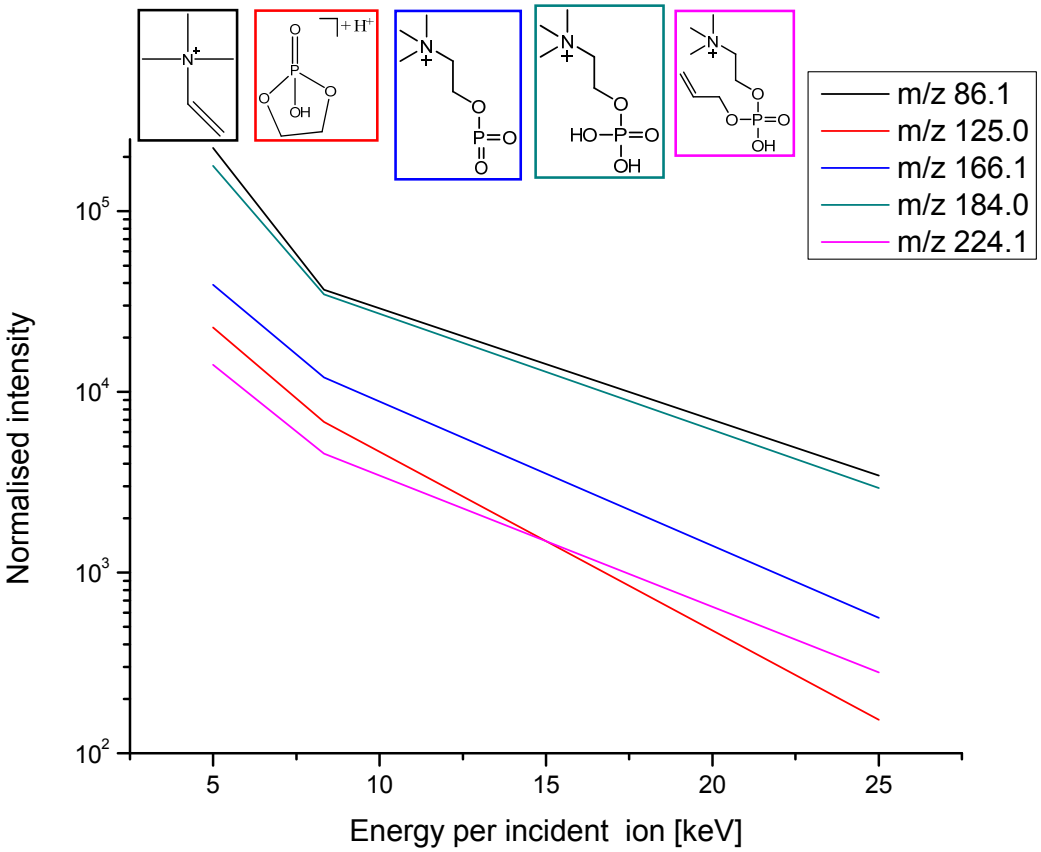

Figure 3.22: *Normalised intensities of different characteristic fragment ions in the low mass range as a function of the energy per incident atom for Bi_n^+, n= 1, 3, 5. Above the diagram the structures of the characteristic fragment ions are shown.*

A reduced energy per incident ion increases also the intensity of large fragment ions. Therefore the intensity of the "C" fragment ions at m/z 478.3 can be increased by a factor of 100, when Bi_5^+ instead of Bi_1^+ is used. The protonated molecular ion can only be detected with poly-atomic primary ions; otherwise the high energy of the Bi_1^+ atoms will enable the fragmentation and dissociation of the precursor ion. In Figure 3.23 the influence of different primary ions on the intensity from the precursor and fragment ions is demonstrated.

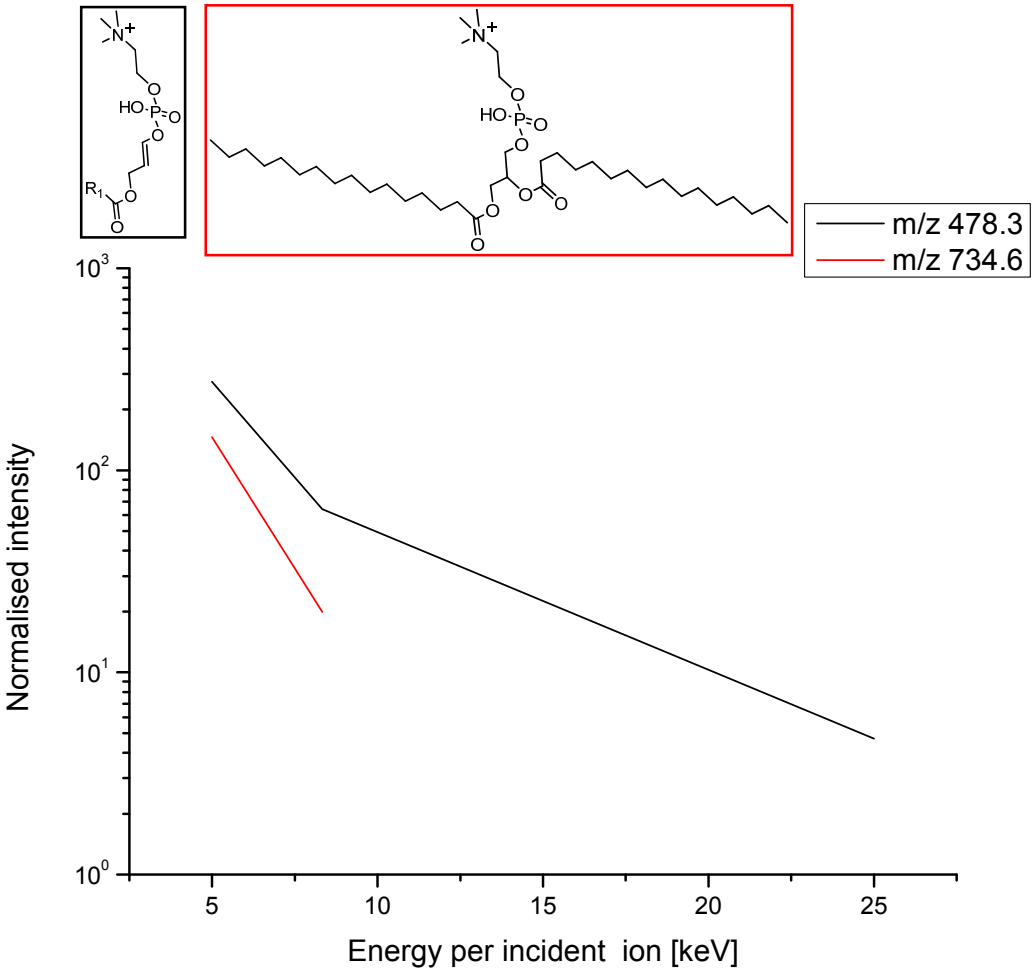

Figure 3.23: *Normalised intensities of different characteristic fragment ions in the high mass range as a function of the energy per incident atom for Bi_n^+, n= 1, 3, 5. Above the diagram the structures of the characteristic fragment ions are shown.*

With the ToF-SIMS instrument it is also possible to use double charged primary ions. Multiple charged primary ions do not influence the fragmentation and ionisation process in such a way that a significant enhancement of the fragment ions in the higher mass area is reached. For the most fragment ions it is no difference between the double and single charged primary ions. This is illustrated in Figure 3.24 for the PC 16:0-16:0. Only the intensity of the protonated molecule ion of the phospholipid can be increased when Bi_3^{++} instead of Bi_1^+ is used.

The reason why small primary ions are preferred for surface spectra than poly-atomic ions is that the measuring time for a specific primary ion dose will dramatically increase, because the higher bismuth primary ions have less ion currents and therefore more time is needed until the same ion dose of a mono-atomic primary ion is reached.

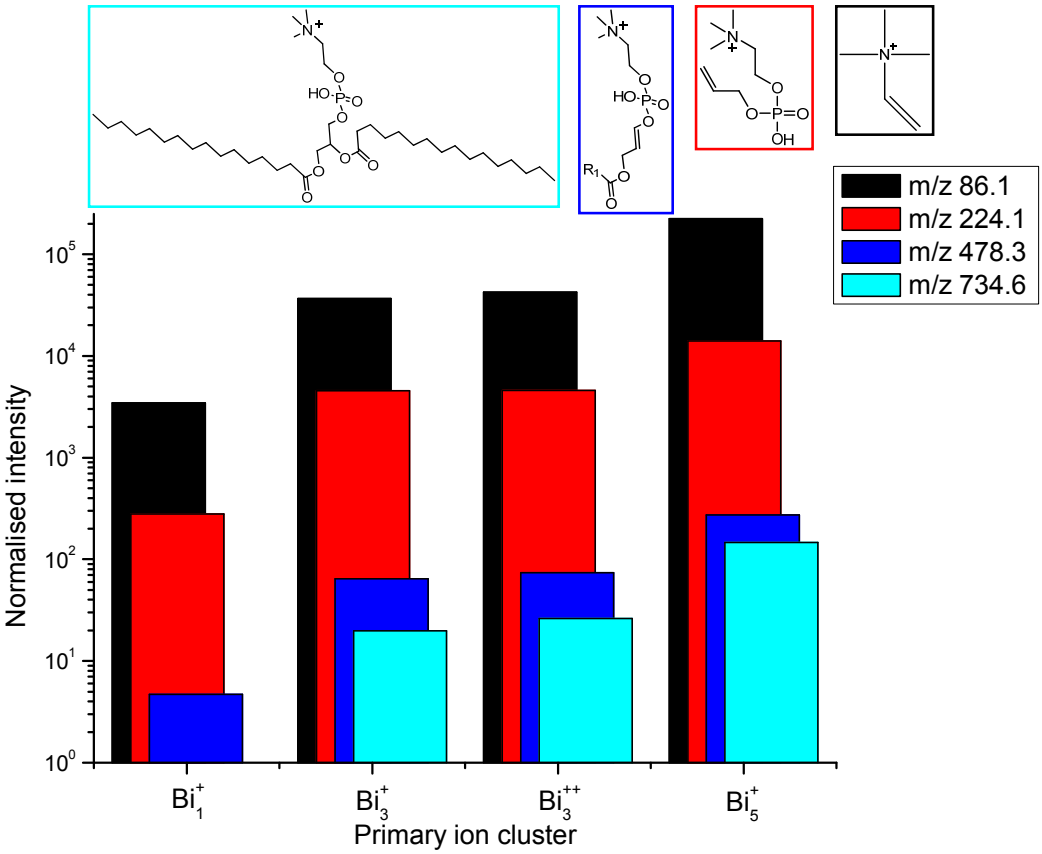

Figure 3.24: *Normalised intensities of different characteristic fragment ions as a function of the different primary ions (Bi_n^+, n= 1, 3, 5 and Bi_3^{++}).*
Above the diagram the structures of the characteristic fragment ions are shown.

3.4 Spectral Characterisation of 1,2-Di-O-hexadecyl-glycero-3-phosphocholine

3.4.1 Sample preparation

The glycerophospholipid namely 1,2-Di-O-hexadecyl-glycero-3-phosphocholine (abbreviation PC O 16:0-16:0) is commercially available (P-1527, Sigma-Aldrich, Austria). The lipid was stored at any time in a dark glass vial with Teflon septa and in a freezer at -18°C, except for preparing the sample solution.
For further analyses a lipid stock solution was prepared. Therefore 0.50 mg of the lipid were dissolved in 500 µL of a methanol-trichloromethane mixture (CH_3OH:$CHCl_3$ = 8:2). Therefore a commercially available methanol (34885, Sigma-Aldrich, Austria) and trichloromethane (288306, Sigma-Aldrich, Austria) were used. After that the dissolving process was completed by ultra-sonification for five minutes.

For the MALDI-ToF measurements[1] 2',4',6'-Trihydroxyacetophenone (91928, Sigma-Aldrich, Austria) as matrix was used. Again a stock solution of 10 mg 2',4',6'-Trihydroxyacetophenone (THAP) in 1000 µL methanol was prepared for all analyses and ultra-sonicated for 5 minutes to have a homogenous solution.
The MALDI-MS spots were prepared with the dried-droplet technique. Therefore 10 µL of the THAP stock solution and 10 µL of the lipid stock solution were homogenised in an Eppendorf tube. Then a MALDI target was cleaned by rinsing several times sequential with acetone (650501, Sigma-Aldrich, Austria) and 2-propanol (34965, Sigma-Aldrich, Austria).
After that 0.8 µL of the solution in the Eppendorf tube was transferred on a sample spot of a stainless steel target and the organic solvent was allowed to evaporate.

[1] in co-operation with E. Pittenauer, research group of (Bio)Polymer Analysis, Institute of Chemical Technologies and Analytics, Vienna University of Technology

This procedure was repeated several times so that at least five spots were available for the MALDI-TOF measurements. After preparation the target was introduced immediately into the vacuum chamber of the instrument.

Prior the preparation for the TOF-SIMS measurements the Si 111 wafer (Infineon, Austria) was carefully cleaned by ultra-sonification in a standard piranha etch solution (H_2O_2 : H_2SO_4 = 1 : 3; H_2O_2: 18312, Sigma-Aldrich, Austria; H_2SO_4: 84720, Sigma-Aldrich, Austria) and rinsed afterwards sequential with MilliQ-water (18.2 $M\Omega cm^{-1}$) and 2-propanol.
Then the silicon wafer was dried with high purity nitrogen. After that 5 µL of the lipid stock solution was placed with a pipette on the clean silicon wafer and the organic solvent was allowed to evaporate.
The deposition process was carried out in a laminar air flow box in order to prevent airborne particulate contamination. Finally the sample was mounted on the back mount sample holder and introduced immediately after preparation into the vacuum chamber of the instrument.

3.4.2 MALDI-ToF measurements results and discussion

The full MALDI-ToF spectrum (see Figure 3.25) of 1,2-Di-O-hexadecyl-glycero-3-phosphocholine (abbreviation: PC O 16:0-16:0) indicate three different possible precursor ions at m/z 706.6, m/z 728.6 and m/z 744.6. The first ion at m/z 706.6 is the protonated molecular ion of PC O 16:0-16:0. The ions at m/z 728.6 and m/z 744.6 are the sodium and potassium adduct ions of the molecular ion.

The substance class of phosphocholine is proofed with the fragment ion at m/z 86.1. This fragment ion consists of a quaternary amino group and is a well-known marker for the choline group.
A direct identification of the whole phosphatidyl group is not possible, because the specific fragment ions at m/z 224.1, m/z 184 and m/z 166.1 are missing (see fragmentation scheme in Figure 3.28 and 3.29).

The very intense fragment ions at m/z 169.1, m/z 191.1 and m/z 207.0 are not related to the phospholipid. They are the corresponding fragment ions for the used MALDI-matrix of 2',4',6'-Trihydroxyacetophenone. Again the ion at m/z 169.1 is the protonated molecular ion peak. The other two peaks are the sodium and potassium adduct ions of the matrix.

The rest of the fragment ions of the lipid are not characteristic cleavage fragments from one of the precursor ions, because they were built through uncontrolled fragmentation processes.

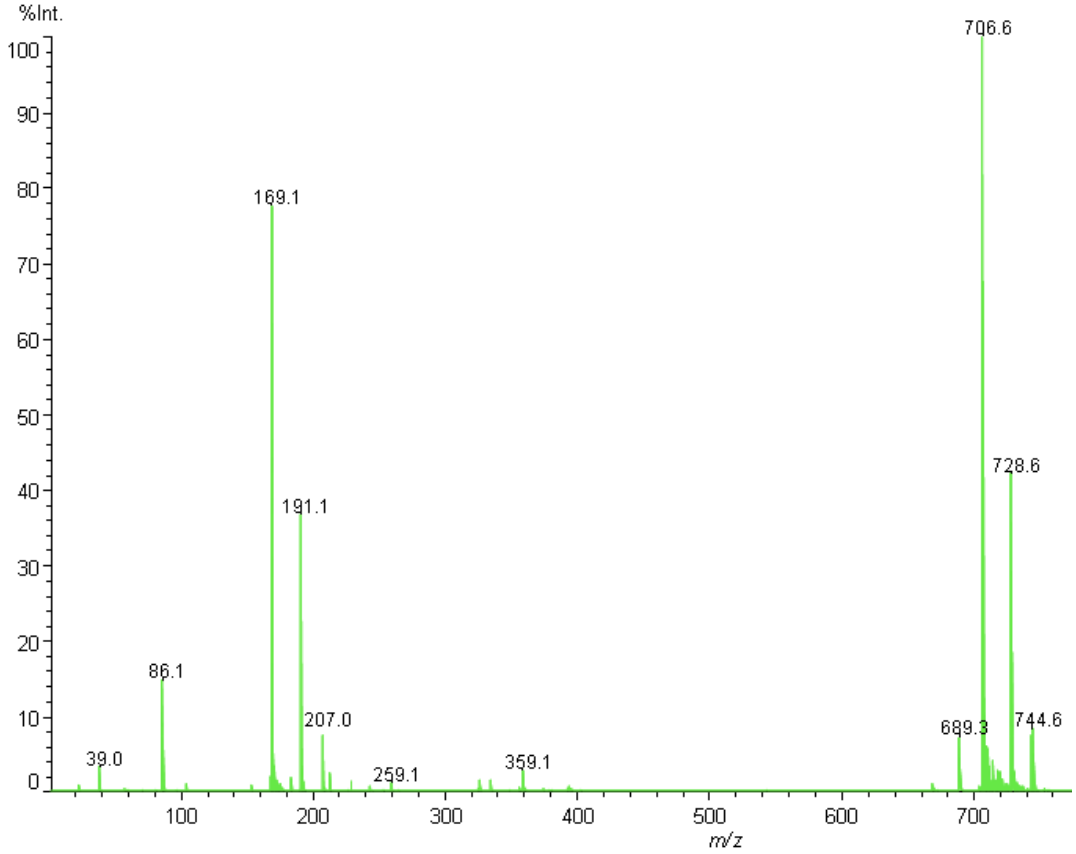

Figure 3.25: *Positive full MALDI-ToF spectrum of 1,2-Di-O-hexadecyl-glycero-3-phosphocholine (PC O 16:0-16:0)*

For characterisation of the glycerophospholipid a MALDI-ToF MS/MS collision induced decomposition (CID) experiment was done. Therefore the protonated molecular ion of the lipid was used as a precursor ion and the ion gate was set symmetrically at m/z 706.6 +/- 2.

Based on these results a systematic structural elucidation from the precursor ion at m/z 706.6 is possible. For the spectrum see Figure 3.26.

The fragment ions in the range of m/z 540 to m/z 690 are characteristic for the cleavage of one carbon atom at the end of the fatty acid group. In the process an olefin structure of the fatty acid is formed and a fragment ion of m/z 16 is eliminated.

The fragment ion at m/z 480.3 is a unique characteristic fragment ion for the glycerophospholipid. This ion determines not only the type of phospholipid, but it is also unique for the fatty acids of the lipid.
The fragment ion indicated the partially loss of one fatty acid in a way that a carbonyl group remains on the fragment ion. If the lipid has different fatty acids two fragment ions at different masses will be formed.

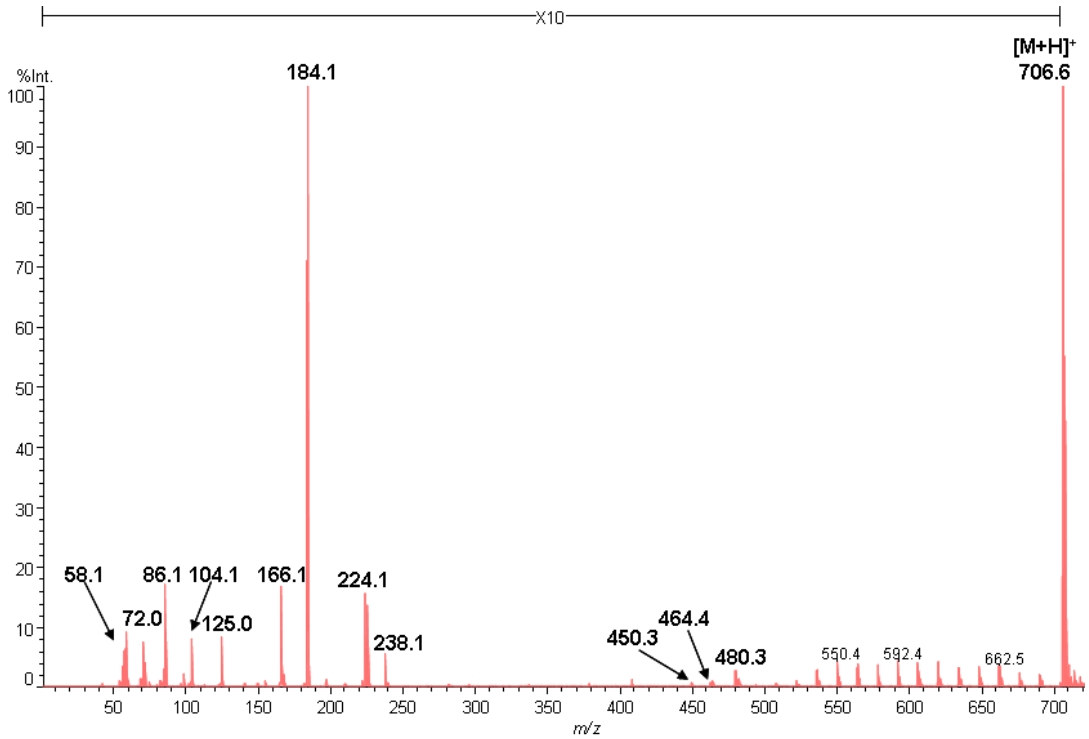

Figure 3.26: *Positive MALDI-CID spectrum of 1,2-Di-O-hexadecyl-glycero-3-phosphocholine (PC O 16:0-16:0) from the precursor ion at m/z 706.6*

For the PC O 16:0-16:0 the fragment ions at m/z 464.4 and m/z 450.3 are additional fragmentation products to the ion at m/z 480.3. One of the fatty acid is in both cases eliminated and only two different olefin structures are formed.

If the fatty acid is completely eliminated from the lipid then the fragment ion at m/z 238.2 is resulting. The fragment ion has also lost the ether functionality in the molecule. Only one carbonyl group is remaining on the molecule where, at the protonated molecule ion on position 1, the long-chain aliphatic hydrocarbon chain was.

The equivalent "G" fragment ion at m/z 224.1 has a complete loss of the fatty acids functions and determines only the type of phospholipid, because it consists of the glycerol and phosphocholine functionalities. The next fragment ions which occur in the spectrum at m/z 184.1 and m/z 166.0 are specific losses of the complete glycerol group labelled with "G – 40" and additionally one oxygen atom of the phosphoric acid ester group which results in the "G - 58" fragment ion.

In the lower mass range there are also some characteristic fragment ions which are not part of the used nomenclature. The protonated fragment ion at m/z 125.1 is a rearrangement of the phosphoric acid ester group. It determines the phospholipid class accurately, because of the low and odd-numbered molecular mass. (Remark: This ion is the only odd-numbered fragment ion of the spectrum.) The fragment ion at m/z 104.1 contains a quaternary amino group and indicates the choline functionality of the lipid.

The next two fragment ions at m/z 86.1 and m/z 72.1 are signalling molecules for the choline group which are built after complete cleavage of the phosphoric acid from the phosphocholine group. The fragment ion at m/z 58.1 is a quaternary amino group which has lost the rest of the glycerophospholipid.

The spectral characterisation with the MALDI-ToF technique was completed with a MALDI-ToF MS/MS post source induced decay (PSD) experiment. For the PSD experiment the same instruments settings as for the CID experiment was used without the helium as collision gas.
The protonated molecular ion of the lipid was selected as a precursor ion and the ion gate was set symmetrically at m/z 706.6 +/- 2.

The PSD spectrum of the lipid PC O 16:0-16:0 is shown in Figure 3.27. The mass at m/z 706.6 is the protonated molecular ion of the glycerophospholipid. The fragment ion at m/z 464.4 has lost completely one fatty acid chain and is characteristic for the ether bond glycerophospholipid.

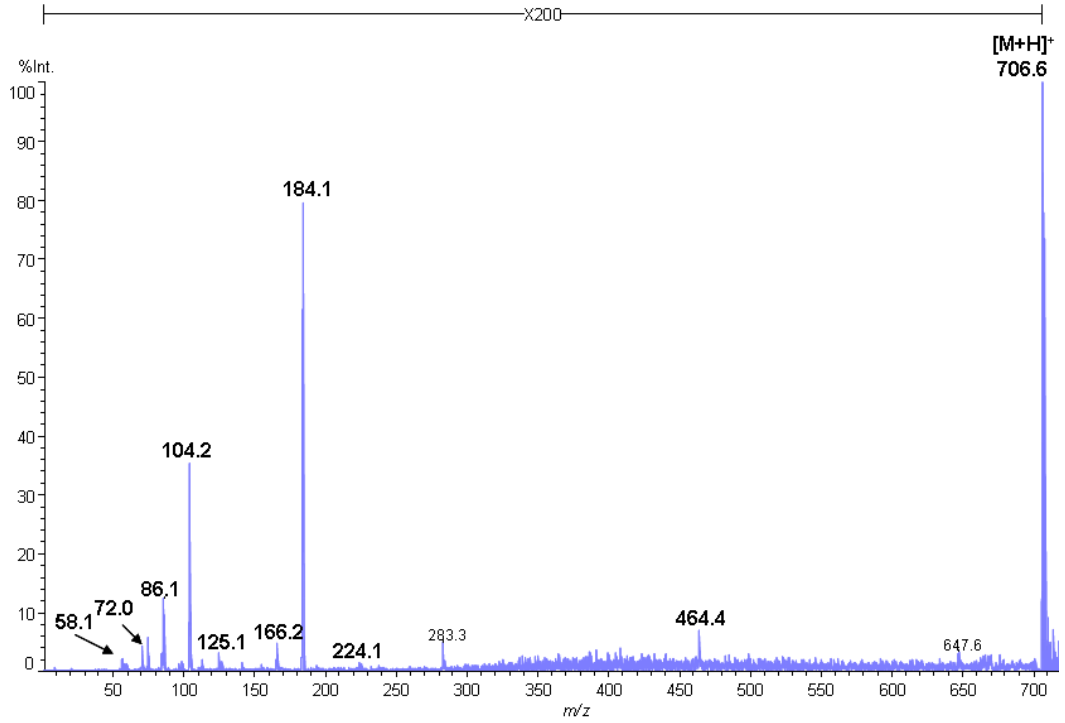

Figure 3.27: *Positive MALDI-PSD spectrum of 1,2-Di-O-hexadecyl-glycero-3-phosphocholine (PC O 16:0-16:0) from the precursor ion at m/z 706.6*

For the characterisation of the phospholipid type the fragment ion of m/z 184.1 can be used. The two fatty acids groups and the glycerol group of the lipid are completely lost and the fragment ion is only the phosphoric acid ester of the choline.

The next fragment ions which occur in the spectrum at m/z 166.2, and m/z 104.2 are specific losses of the complete glycerol group. The protonated fragment ion at m/z 125.1 is a rearrangement of the phosphoric acid ester group. The next two fragment ions at m/z 86.1 and m/z 72.1 are the signalling molecules for the choline group and the fragment ion at m/z 58.1 is a quaternary amino group which has lost the rest of the glycerophospholipid.

More characteristic fragment ions are not detected in the PSD spectrum, because the selected precursor ions have no collision with other atoms or ions through the flight time in the time-of-flight section of a PSD experiment. Therefore only metastable ions which are formed spontaneously from the precursor ion can be detected in this experiment.

The following Figures 3.28 and 3.29 describe the fragmentation scheme of the whole fragment ions which were detected through the CID experiment. The fragmentation scheme gives also an overview about the structural elucidation of the different fragment ions.

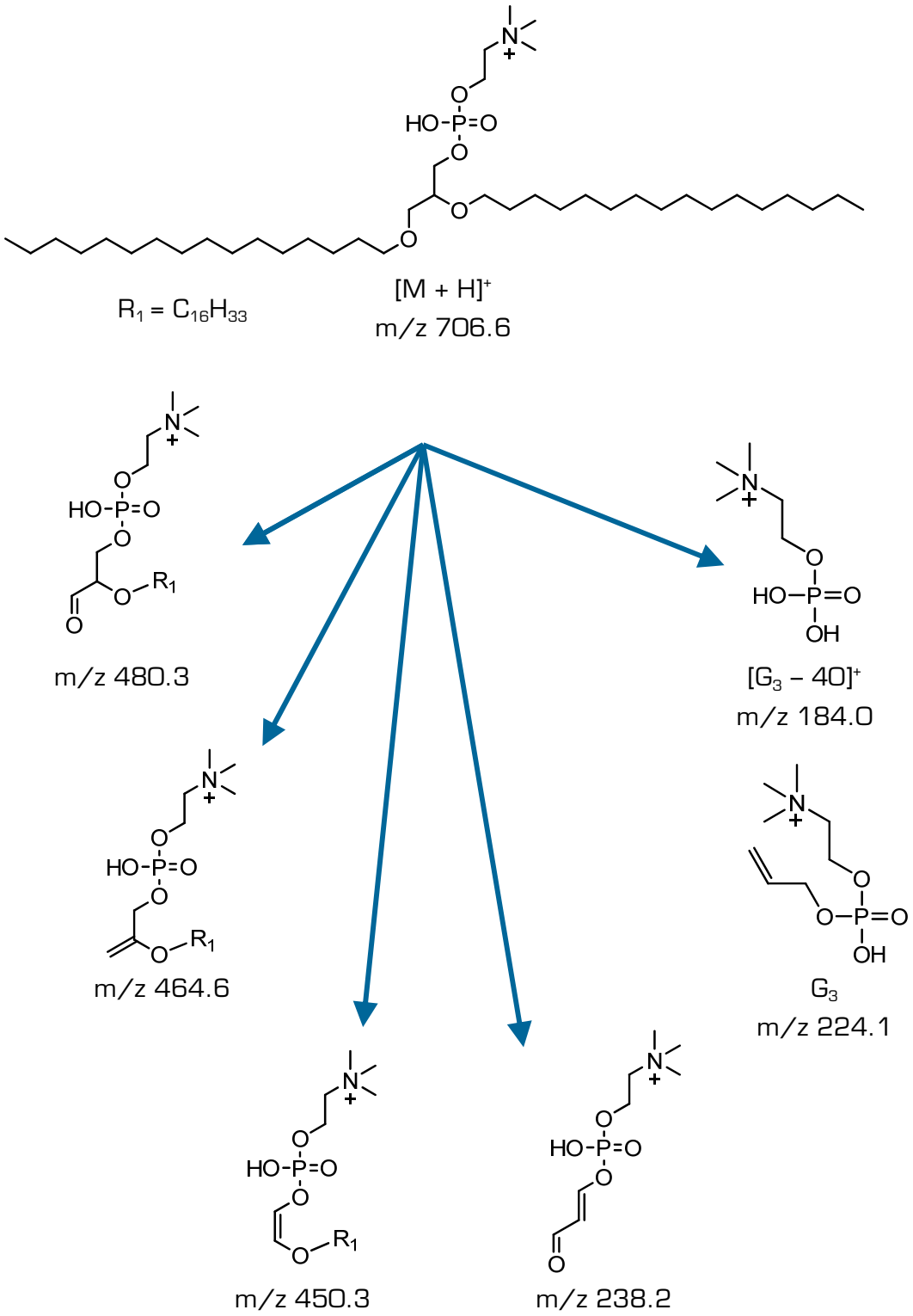

Figure 3.28: *Fragmentation scheme of PC O 16:0-16:0 for the characteristic fragment ions in the high mass range*

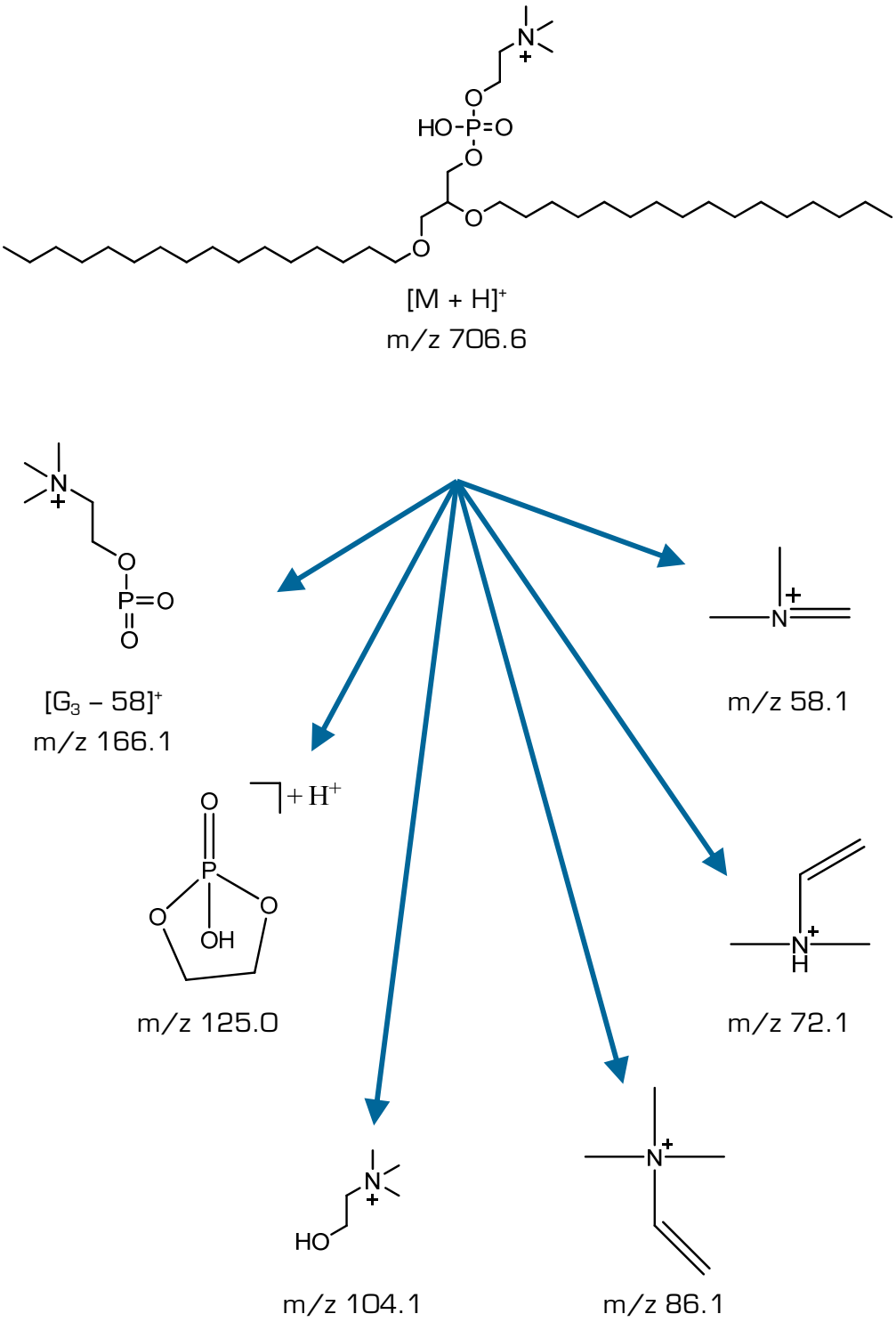

Figure 3.29: *Fragmentation scheme of PC 016:0-16:0 in the low mass range*

3.4.3 ToF-SIMS measurements results and discussion

The positive ToF-SIMS mass spectrum observed for PC O 16:0-16:0, which is shown in Figure 3.30, reveals only a protonated molecule ion at m/z 706.6. All other weak fragment ions are not characteristic adduct ions in comparison to the MALDI-ToF spectrum (see Figure 3.25). In contrast to the other two lipids the detected molecular ion can be used for characterisation or imaging experiments of the lipid, because the intensity therefore is high enough.
The characteristic fragment ion at m/z 480.3 has partially lost one fatty acid chain. The fragment ions at m/z 464.3 and 450.3 contain only one fatty acid chain and are different in the way the ether functionality is eliminated. The last two characteristic fragment ions can be used for identifying the whole glycerophospholipid, because one of the fatty acid functionality is remaining on the molecule.
When both fatty acid chains are complete lost, then the very weak fragment ion at m/z 238.2 is formed.

In the region of the low masses the fragment ions at m/z 224.1, m/z 184.2 and m/z 166.1 are characteristic for the phospholipid type. The fragment ion at m/z 224.2 has beside the phosphocholine group also a bonding to the main alcohol (in that case to glycerol).

According to the MALDI-CID spectrum also characteristic fragment ions for the phosphoric acid and amino group are generated. For the 5-membered phosphor heterocycle the ion at m/z 125.1 is formed. The ions at m/z 104.1, m/z 86.1, m/z 72.1 and m/z 58.1 contain a quaternary amino group and indicate the choline functionality of the lipid.

For the fragmentation scheme see Figure 3.28 and 3.29. The additional molecular formula for the fragment ion at m/z 104.2 is shown in Figure 3.11.

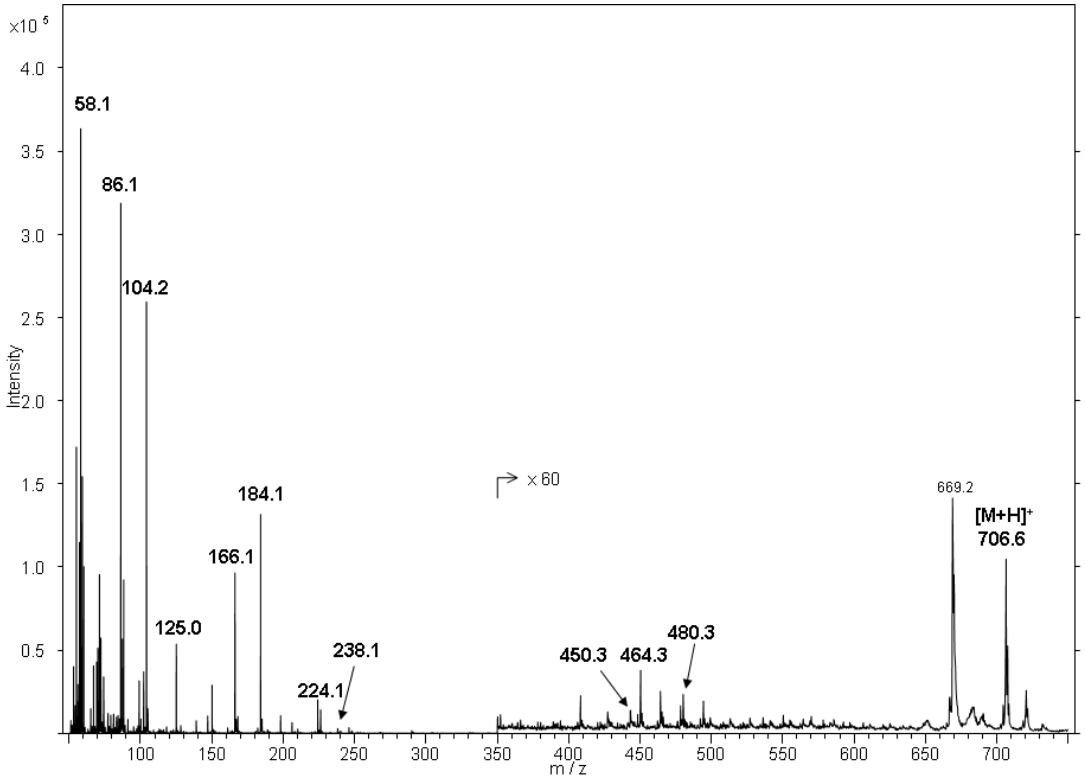

Figure 3.30: *Positive ToF-SIMS spectrum of PC 0 16:0-16:0 on a clean silicon wafer surface with* Bi_3^{++} *as incident primary ion with an acceleration voltage of 25kV*

In contrast to the full MALDI-ToF and to the MALDI-PSD spectra (see Figure 3.16 and 3.18) it is demonstrated that with the help of the ToF-SIMS technique it is possible to have access to most of the characteristic fragment ions, so that an accurate determination of the different glycerophospholipids is possible.

For the PC 0 16:0-16:0 the dependency between the type of the primary ion and the intensity of the characteristic fragment ion is illustrated in Figure 3.31. The interaction of primary ions with the organic target molecules is depending on several processes which are not completely determined at all. In a first approximation an energy transfer of the kinetic energy of the primary ion to the organic target molecule is done. Therefore poly-atomic primary ions will cause different fragmentation and ionisation processes of the glycerophospholipid.

When mono-atomic primary ions are used then the large organic molecule is nearly complete fragmented. If poly-atomic primary ions interact with the organic target molecule then the fragmentation process can be decreased, because of the lower energy per single incident ion. The Figure 3.31 shows that incident ions with reduced energies increase the intensity of lager characteristic fragment ions.

The interesting fact is that in contrast to the fatty acid ester lipids the protonated molecule ion is formed easily with a high intensity also with mono-atomic ions as projectiles. The second difference is that the increasing of the intensity for different primary ions is not so distinctive like at the other lipids.

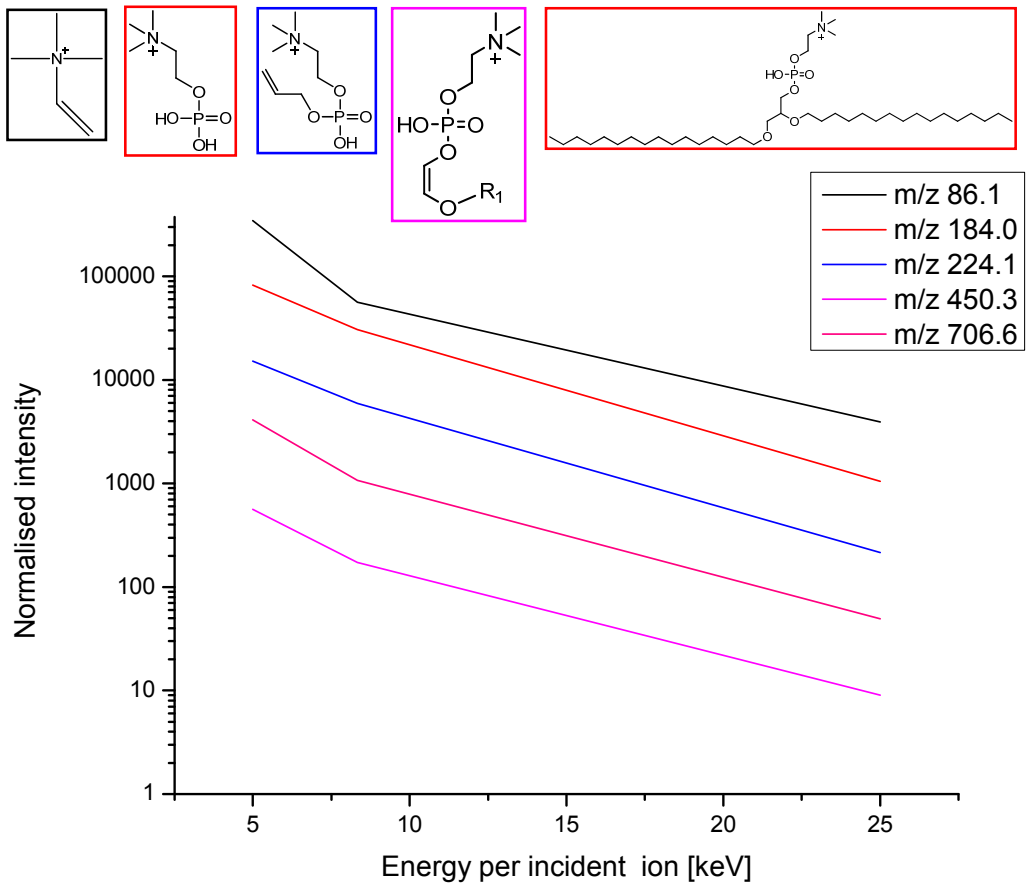

Figure 3.31: *Normalised intensities of different characteristic fragment ions as a function of the energy per incident atom for Bi_n^+, n= 1, 3, 5. Above the diagram the structures of the characteristic fragment ions are shown.*

A reduced energy per incident ion increases also the intensity of large fragment ions. Therefore the intensity of the fragment ion at m/z 224.1 can be increased by a factor of 100, when Bi_5^+ instead of Bi_1^+ is used. The protonated molecular ion can exactly be detected with poly-atomic primary ions; otherwise the high energy of the Bi_1^+ atoms will enable the fragmentation and dissociation of the precursor ion. In contrast to the ester bound lipids it is also possible to use the protonated molecular ion.
In Figure 3.31 the influence of different primary ions on the intensity from the precursor and fragment ions is demonstrated.

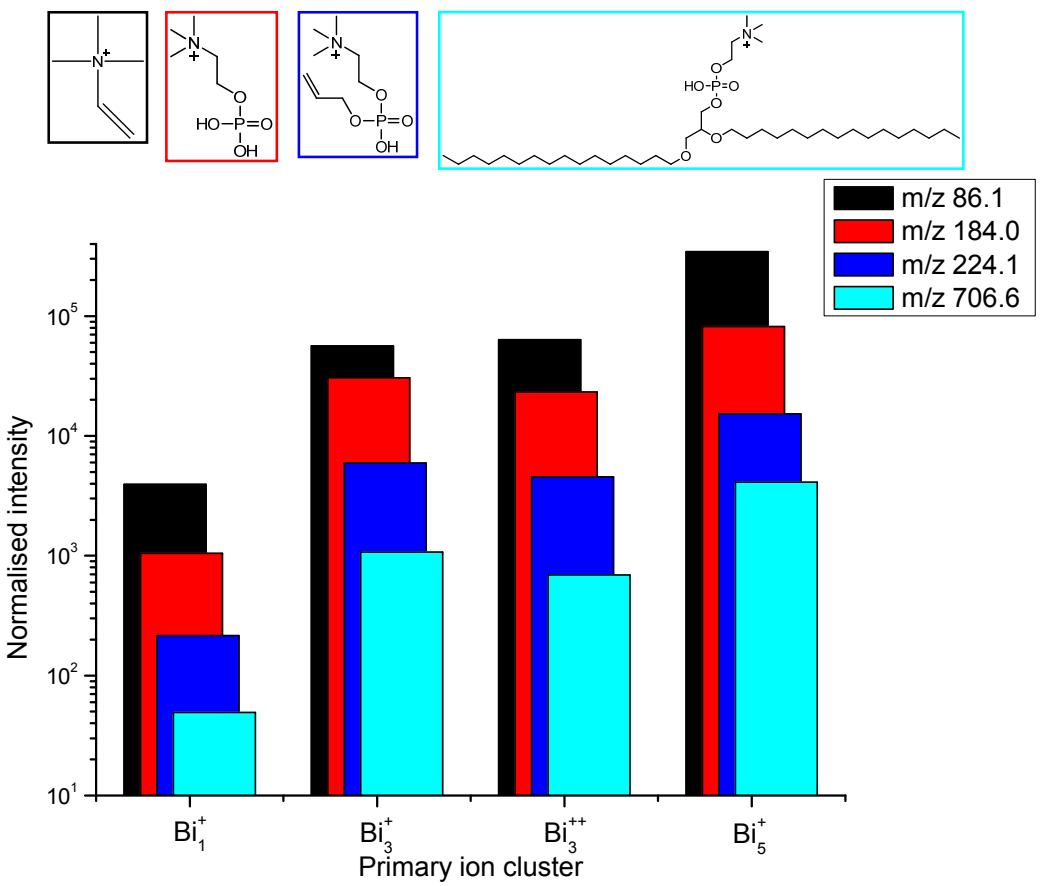

Figure 3.32: *Normalised intensities of different characteristic fragment ions as a function of the different primary ions (Bi_n^+, n= 1, 3, 5 and Bi_3^{++}).*
Above the diagram the structures of the characteristic fragment ions are shown.

With the ToF-SIMS instrument it is also possible to use double charged primary ions. Multiple charged primary ions do not influence the fragmentation and ionisation process in such a way that a significant enhancement of the fragment ions in the higher mass area is reached. For the most fragment ions it is no significant difference between the double and single charged primary ions. This is illustrated in Figure 3.32 for the PC O 16:0-16:0. Only the intensity of the protonated molecule ion of the phospholipid can be increased when Bi_3^+ instead of Bi_3^{++} and Bi_1^+ is used.

The reason why small primary ions are preferred for surface spectra than poly-atomic ions is that the measuring time for a specific primary ion dose will dramatically increase, because the higher bismuth primary ions have less ion currents and therefore more time is needed until the same ion dose of a mono-atomic primary ion is reached. The advantage of poly-atomic primary ions is that the partial surface damage is drastically reduced and therefore more molecule ions can be ionised and detected.

Chapter 4

Conclusion

The investigation of the outermost monolayers of surfaces is a difficult and demanding analytical task for the modern organic mass spectrometry. A strong fragmentation and the missing possibility for MS/MS experiments at the ToF-SIMS instrument don't allow an accurate interpretation of mass spectra of phospholipids.

The present study demonstrates that with the help of the structural elucidation of phospholipids with the MALDI MS technique all of the possible characteristic fragment ions can be identified. Then the mass spectrum of the complex organic molecules can be interpreted with the knowledge of the MALDI experiments. The advantage of the ToF-SIMS spectra is now that images of the phospholipid distribution of a biological tissue section for example can then easily be created with a high spatially resolution. Therefore the characteristic fragment ions are used instead of the protonated molecule ions to differentiate between the single phospholipids.
In this work also the influence of poly-atomic primary ions at the ionisation and fragmentation principle is shown. The analyte signal of fragment ions in the high mass range increased by using Bi_5^+ instead of Bi_3^+ and Bi_1^+. There is only a slight improvement of the intensity when the Bi_3^{++} ion as primary cluster is used (except in the case of the ether bound glycerophosphatidyl-choline).
This dependency can be illustrated by comparing the total ion yield for every primary ion type. The total ion yield Y_{tot} is calculated through normalisation of the total number of secondary ions N_{Sl} to the quantity of incident primary ions N_{Pl} (see therefore equation 4.1).

$$Y_{tot} = \frac{N_{Sl}}{N_{Pl}} \qquad (4.1)$$

In Figure 4.1 the total ion yield for all of the three different glycerophospholipids is illustrated. With the help of poly-atomic primary ions the total ion yield can be increased through a moderate ionisation and fragmentation process. In addition the energy per incident primary molecule is reduced and therefore the fragmentation of the large secondary ions is decreased. Furthermore the doubled positive charged bismuth cluster (Bi_3^{++}) does not maximise the total ion yield, but partially the intensities of the precursor and characteristic fragment ions are increased.

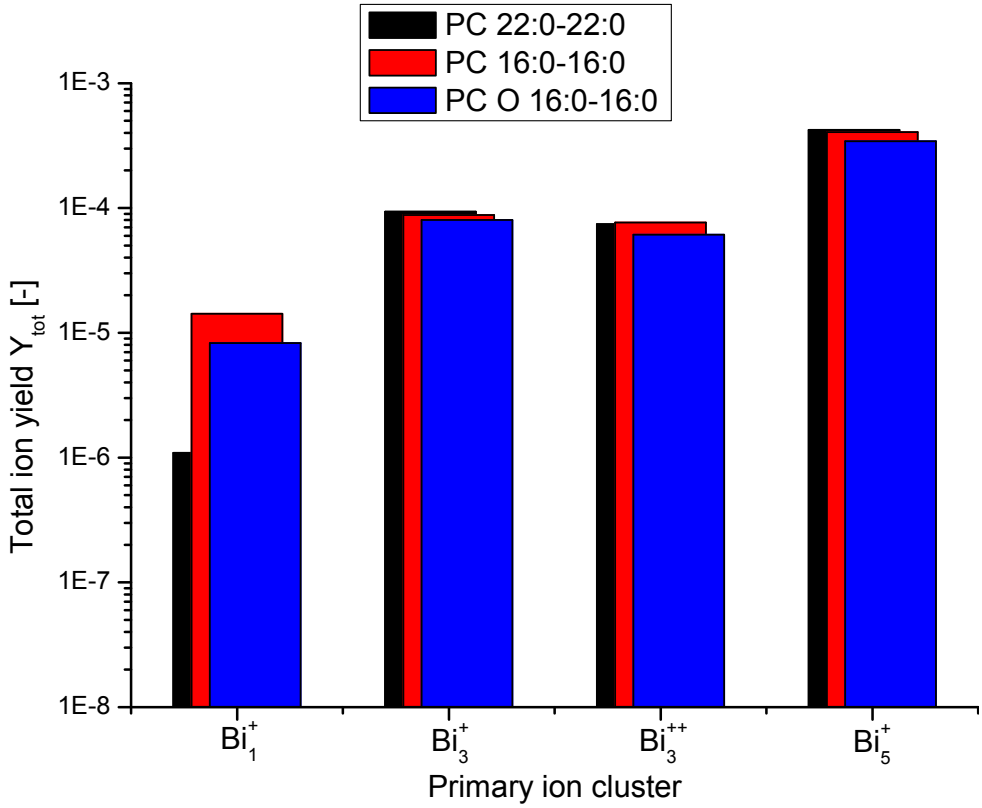

Figure 4.1: *Total ion yield Y_{tot} of the different analysed glycerophosphatidylcholines*

Chapter 5

Maintenance of the bismuth emitter of the LMIG

5.1 Preliminary remarks

The following procedure for maintenance of the bismuth emitter of the liquid metal ion gun (LMIG) was created during the service work on the instrument by our group. The main aim was to have finally a manual which can be easily understand so everybody in Austria can do the necessary steps for maintenance without any language barriers. That is the reason why unfortunately the language of the following pages is German.
All the pictures and described steps are from the originally help file for the TOF.SIMS^5 instrument from Ion-TOF. For details or further information see Literature [24].

5.2 Step-by-step description

Now the changing of the bismuth emitter and the renewal of the optical stack of the primary gun, which is a LMIG, is described in detail in German.

Benötigte Werkzeuge (für Emitter und Ionenoptik):

- Schraubenzieher (verschiedene Größen)
- 13 mm Gabel-/Ringschlüssel
- Inbus-Schraubendreher (0.9 mm)
- Inbus-Schraubendreher (1.0 mm)
- Inbus-Schraubendreher (1.5 mm)
- Pinzetten (mit kleinen runden Spitzen)
- Lupe (1:6)
- Lupe (1:10)
- Emitter Wechsel-Tool (ION-TOF special tool)
- Lens Adjustment Pin (ION-TOF special tool)

1. Belüften der Primärsäule

Mittels „Stop“ in: Instrument → LMIG → Vacuum; Anschlüsse abziehen und mit Abdeckkappen versehen. Abnehmen des Kopfes erst wenn „LMIG“ in FPanel rot leuchtet. Dabei Öffnung an der Gun mit Alufolie abdecken

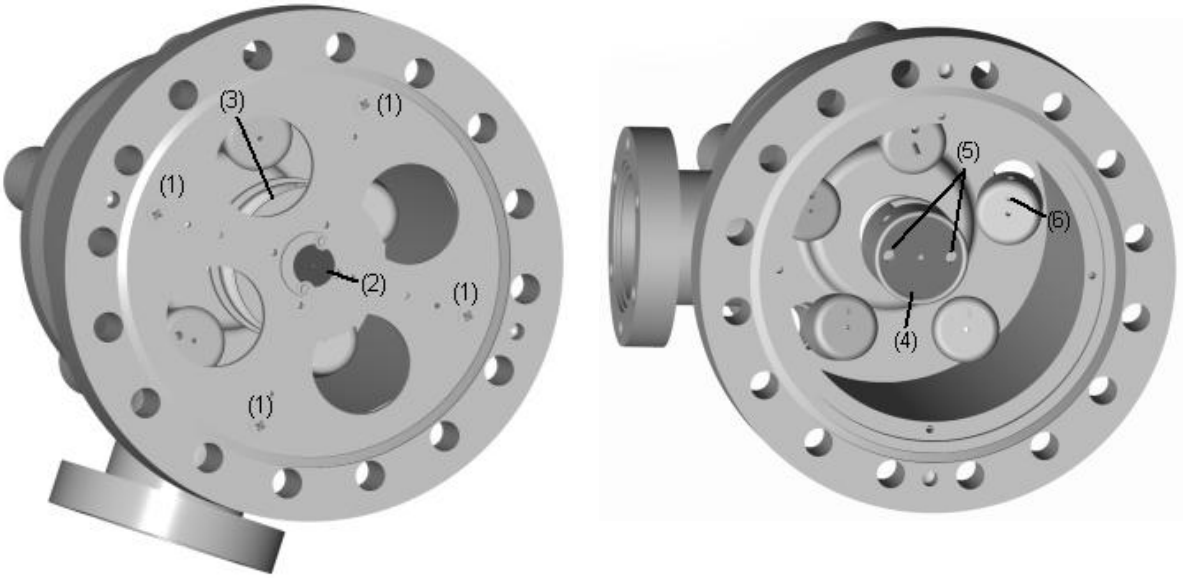

Abb. 1: Frontansicht der LMIG [(1) Kreuzschrauben, (2) Beam defining aperture, (3) optical stack, (4), Suppressor, (5) Suppressorschrauben, (6) Sechskant-schrauben]

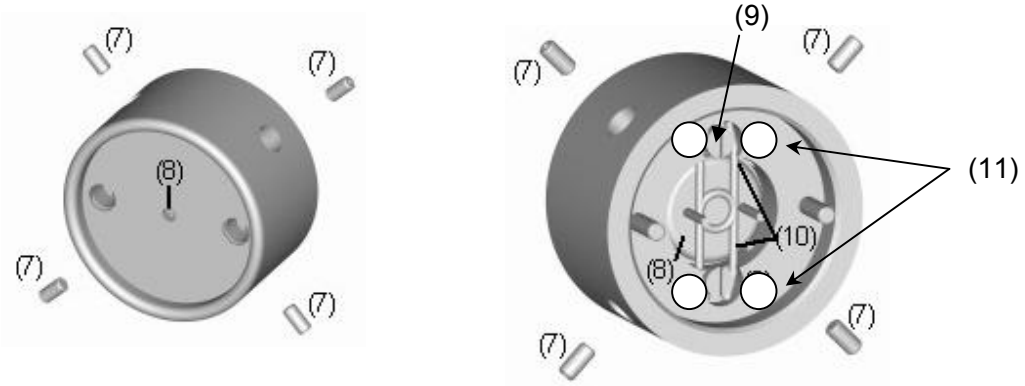

Abb. 2: Frontansicht (links) und Rückansicht (rechts) des LMIG-Suppressors (Typ I) [(7) Emitter-Justageschrauben, (8) LMIG emitter, (9) Emitter clip screws, (10) Emitter clips, (11) Befestigungs-schrauben von oberen und unteren Zylinderteil]

2. *Zerlegen des Primärsäulen-Kopfes (im Kopf ist die Ionenoptik bis zur Beam defining Aperture (siehe Abb. 1, 2)*

- Öffnen der Kreuzschrauben (1)
- Lens Source und Extraktor Anschlüsse zieht man gemeinsam mit dem Linsen/Apertur Stack heraus.
- Öffnen der Schrauben (6) für Filament A, B und Suppressor-Anschlüsse, sowie Herausziehen der Leitungen aus den Anschlüssen
- Lockerung der zwei Suppressorschrauben (5)
- Abnehmen des Emitter-Zylinders mit den zwei Zuleitungen (danach geht es auf dessen Rückseite weiter)
- Entfernen der beiden Heating Drähte
- Lockerung der vier Justageschrauben (7)
- Entfernen der Emitter-Clip Schrauben (9) und Emitter-Klammern (10)
- Emitter-Wechsel-Tool auf den gebrauchten Emitter stecken und aus dem Zylinder herausziehen

Optional: Wechseln der Suppressor Apertur (Abb. 1, 2)

- Öffnen der vier Schrauben (11)
- Abnehmen der oberen Zylinderoberseite
- Wechseln der Suppressorapertur
- Zusammenbau des Zylinders in umgekehrter Reihenfolge

3. *Wechseln des Emitters (Abb. 1, 2)*

- Neuen Emitter mittels Emitter-Wechsel-Tool aufnehmen und in Emitterzylinder einsetzen.
- Einsetzen der Klammern (10) und befestigen dieser mittels Schrauben (9). Die Schrauben (9) dabei vorsichtig anziehen, damit die Keramik-Halterung nicht zerstört wird.
- Emitter-Wechsel-Tool wieder abnehmen
- Zylinder umdrehen.

- Ausrichten bzw. Zentrieren des Emitters:

  Dabei mit dem Zylinder unters Mikroskop!
  Mittels zweier 0.9 Zoll Inbus-Schraubendreher kann man den Emitter in X und Y Richtung mit den Justierungsschrauben (7) ausrichten. Dabei je nach belieben die Schraubenziehen gegenüber einsetzten und gleichzeitig nach vor oder zurück drehen oder die Schraubenziehen in 90° Winkel einsetzen und den Emitter bewegen. Wichtig: Die Emitterspitze muss exakt zentral sein, um eine gute Emitterperformance zu erreichen (d.h. gewissenhaft durchführen und mehrmals kontrollieren).
  Nach erfolgter Ausrichtung die Justierungsschrauben anziehen (Achtung: Hier könnte sich der Emitter eventuell noch verschieben, daher nochmals unter dem Mikroskop kontrollieren).

4. Einbau des Emitters in den LMIG Kopf (Abb. 1, 2)

- Emitter-Zylinder wieder umdrehen und Heizdrähte wieder einsetzten. Wichtig: Die Drähte dürfen sich nicht kreuzen (sonst entsteht ein Kurzschluss).
- Einsetzen des Zylinders in den Kopf
- Festziehen der zwei Suppressorschrauben (5)
- Einsetzen der Leitungen (FA, FB, SU) in die Anschlüsse
- Schließen der Schrauben (6) für Filament A, B und Suppressor Anschlüsse
- Den Linsen/Apertur-Stack nun in den LMIG Kopf einsetzen. Dabei die Drähte für Lens Source und Extraktor gewissenhaft auf den dafür vorgesehenen Anschlüssen befestigen. Dieser Schritt kann mehrere Versuche benötigen
- Die Schrauben (1) anziehen
- Gesamten Stack mehrmals mit Luft ausblasen

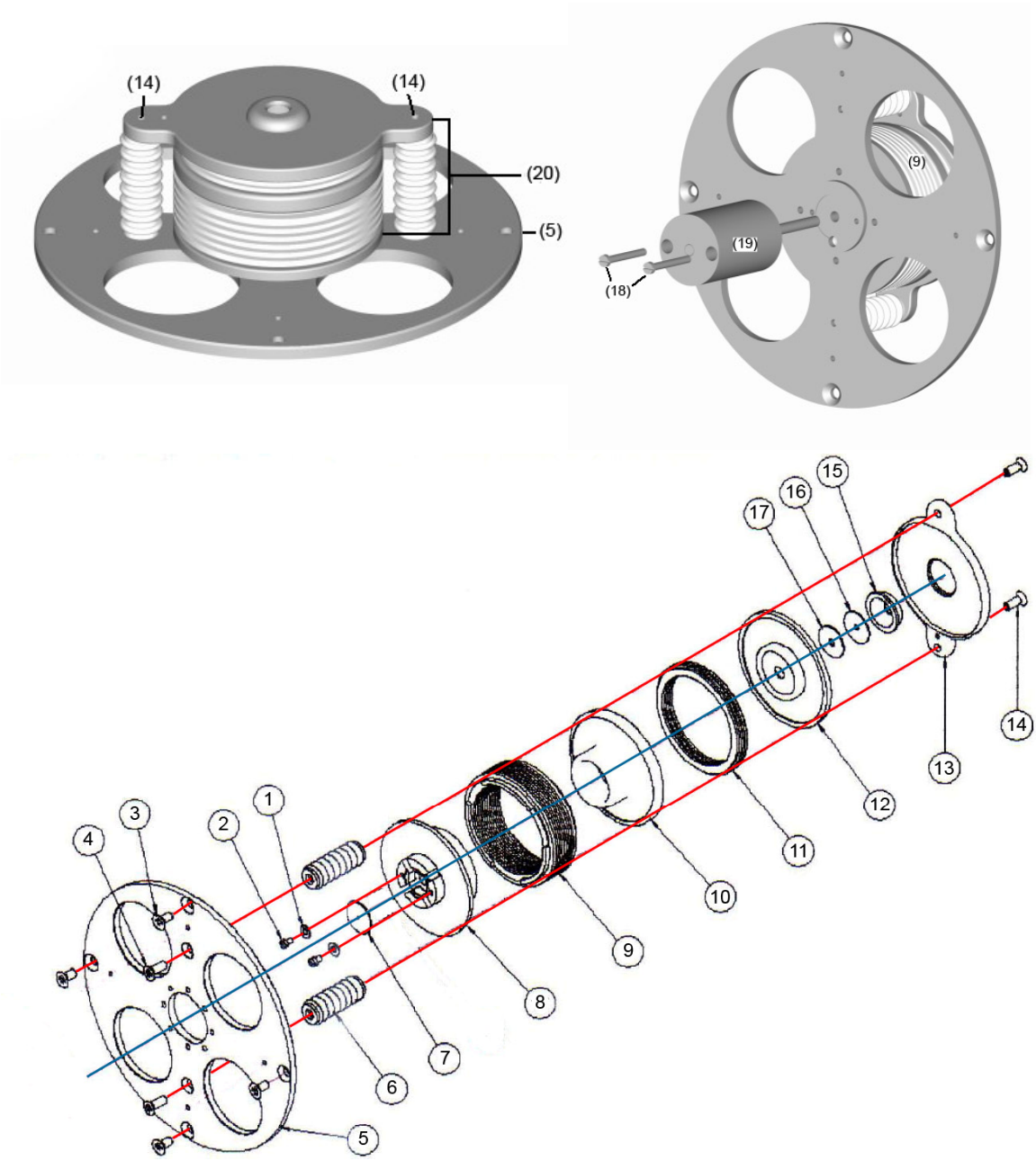

Abb. 3: Ionenoptik der LMIG (oben Seitenansicht und unten Detailansicht) [(1) Beilagscheibe zur Fixierung der Beam defining aperture, (2) Schrauben zur Fixierung der Beam defining aperture, (3) Schrauben zur Fixierung der Ionenoptik an der LMIG Säule, (4) Schrauben zur Befestigung der Linsen an die Basisplatte, (5) Basisplatte, (6) Isolierung, (7) Beam defining aperture, (8) Lens Out, (9) Lens ceramic 46 x 16, (10) Lens center, (11) Lens ceramic 44 x 5, (12) Lens in, (13) Lens clamp, (14) Schrauben zur Befestigung der Linsen an die Lens clamp, (15) Extractor, (16) Extractor aperture (silber), (17) Lens protection aperture (schwarz), (18) Schrauben zur Befestigung des Justage-Tools, (19) Lens Adjustment Pin (Ion-TOF special tool)]

Optional: Zerlegen der Ionenoptik für den Wechsel von Apertur, Isolatoren oder Linseneinheiten (Abb. 3)

- Bei Bedarf kann auch die gesamte Ionenoptik gereinigt werden. Siehe dazu die entsprechende Anleitung.
- Durch Entfernen der Schrauben (14) auf einer Seite kann der ionenoptische Teil leicht zerlegt werden.
  Dabei ist auf die Ausrichtung der elektrischen Verbindungen (Extractor und Lens Source) zu achten.

Optional: Zusammenbau und Zentrierung der Ionenoptik nach dem Wechsel (Abb. 3)

- Die Isolierung (6) mit den Schrauben (4) an der Basisplatte (5) fixieren. Dabei die Schrauben nicht komplett festziehen.
- Entfernen der Beam Defining Aperture (7) durch die Schrauben (2)
- Einsetzen des Lens Adjustment Pin (19) und mit (18) an (5) festschrauben
- Zusammensetzen der Linse (dazu Teile (8), (9), (10), (11) und (12) zusammenbauen). Beim Zusammenbau die Teile mit Luft abblasen, um kleine Partikel zu entfernen
- Einbau der beiden Extraktor-Aperturen. Zuerst (17), dann (16) auf (12) legen. Es ist wichtig, dass zuerst die Kohlenstoffblende (schwarz, 17) und dann erst die Metallblende (silbrig, 16) auf der Lens in – Elektrode (12) zum Liegen kommt.
- Auf die Metallblende (16) wird der Extractor (15) aufgesetzt.
- Aufsetzen der Lens clamp (13) auf den Isolatoren (6) und Festziehen der Schrauben (14)
- Montage der elektrischen Zuleitungen (falls abgenommen) für Extractor an (13) und für Lens center an (10)
- Den zusammengebauten Stapel nun in den LMIG Kopf einsetzen. Dabei die Drähte für Lens Source und Extraktor gewissenhaft auf den dafür vorgesehenen Anschlüssen befestigen. Dieser Schritt kann mehrere Versuche benötigen
- Die Schrauben (3) anziehen
- Die beiden Schrauben (4) nun fest anziehen
- Lens Adjustment Pin (19) nach Lösen von (18) wieder entfernen

- Die Beam Defining Aperture (7) durch die Schrauben (2) und Beilagscheiben (1) fixieren.
- Die Ionenoptik ist nun fertig montiert. Am Schluss feststellen, ob die elektrischen Anschlüsse richtig angeschlossen sind.
- Prüfen, ob Kurzschluss zwischen Extractor und Lens Source besteht

5. Aufsetzten des Primärsäulen-Kopfes (Abb. 1, 2)

- Neue CF-Dichtung in den Flansch einsetzen
- Schrauben einsetzten und leicht (aber genügend fest) anziehen. Die Befestigungsschrauben müssen bei seitlichem Durchschauen noch ca. 1 mm sichtbar sein. Dies ermöglicht eine nachträgliche Justage über die Schrauben.
- Anschlüsse richtig anbringen.
- Evakuieren der Säule mittels „Start" in: Instrument → LMIG → Vacuum.
- Fortsetzen erst, wenn Vakuum unter 5E-7 mbar ist (dauert ca. 3 h, wenn möglich über Nacht pumpen lassen.

6. High Potential Tests, Initial Setting

- High Pot Test A und B ausführen, wie im Help File unter Subsystems → LMIG Source → Bismuth (Bi) Source →Maintenance → „High Potential Test" beschrieben. Dabei kann es immer wieder zu Funkenbildung kommen.

  Anm.: *Die Funkenbildung macht sich durch einen roten Balken bzw. Abschalten der Hochspannung bemerkbar. Sollte Test A oder B nach mehreren Versuchen (< 10) nicht erfolgreich abgeschlossen werden können, dann muss die Primärsäule erneut zerlegt und eventuell gereinigt werden (wahrscheinlich sind Partikel oder Verunreinigungen im Strahlengang. Da die Funkenbildung auf einen Fehler in der Isolierung hinweist.)*
- Bi-Emitter wie unter Subsystems → LMIG Source → Bismuth (Bi) Source → Maintenance → „Initial start of a new emitter" beschrieben hochfahren.

- Als nächstes muss der Heizstrom bestimmt werden. Dies ist im Help File unter Subsystems → LMIG Source → Bismuth (Bi) Source → Maintenance → „Determine Heating Current and Extractor value" beschrieben. Entspricht der Kaltstart Prozedur (Methode A *(mit setting file)* oder Methode B *(ohne setting file)*). Der Heizstrom sollte den spezifizierten Wert auf der Emitterverpackung entsprechen. Extraktor und Suppressor sollten nun ebenfalls akzeptable Werte aufweisen.
- Nach der Heizstrombestimmung sollte zur Absicherung noch ein Warmstart (Methode C im Help File) gemacht werde. Dies verbessert die Emitterstabilität. Dabei wird nocheinmal der Heizstrom überprüft und der Suppressor optimiert.

7. Mechanical Alignment on Aperture 1 (Abb. 4)

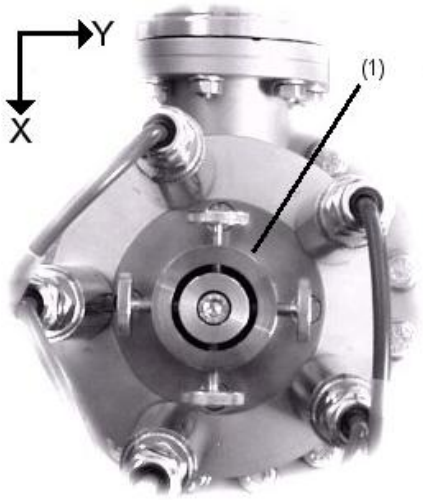

Abb. 4: Frontansicht für die mechanische Ausrichtung

- Folgende Anleitung beruht auf der Hilfeseite:
  - Subsystems → LMIG → Operation → Alignment → „Aligning the beam on aperture 1"
- Die Grobeinstellung erfolgt mittels der Justageschrauben an der Primärsäulenoberseite. Dabei wird die optische Achse grob eingestellt. Ziel ist es dabei, einen minimalen Emissioncurrent zu messen, der vorher über den Suppressor auf 4 µA eingestellt worden ist.

- Nun sicherstellen, dass auf der Apertur 1 ein Strom angezeigt wird (erst dann fortsetzen)
- Emission current auf 2µA mittels Suppressor reduzieren
- Guten Startwert für Lens Source (z. B. vom alten Setting-File) einstellen
- X Source und Y Source auf 0% setzen
- Scope Ap1 betätigen. Width auf 80 % setzen.
- Mittels Justageschrauben nun Emitter in Y-Richtung verschieben, während der Oszilloskop-Scan für die X-Richtung beobachtet wird. Y-Richtung solange verstellen, bis im Bild des Oszilloskop-Scan ein Peak zu sehen ist.
- Mit Center-Schaltfläche Peak zentrieren und Oszilloskop-Width auf 15% herabsetzen und Peak erneut zentrieren.
- Dieselben zwei Schritte für Y-Richtung durchführen (Emitter nun in X-Richtung verstellen, während man die Y-Achse am Oszilloskop-Scan betrachtet)
- X + Y Source sollten dadurch möglichst nahe bei 0 sein. Wenn dies nicht der Fall ist, so hilft bei einer Ablenkung von > 40 – 50% folgende Maßnahme: Flansch-Schrauben an der richtigen Stelle stärker anziehen und anschließend alle Schritte erneut durchführen.
- Nun Lens Source so verändern, dass man einen Rechtecksimpuls sieht.

8. Alignment on the Optical Axis (Abb. 4)

- Folgende Anleitung beruht auf der Hilfeseite:
  - Subsystems → LMIG → Operation → Alignment → „Aligning the emitter on the optical axis“

  Anmerkung: Dieser Schritt dient dazu, den Strahl in die optische Achse zu bringen (bisher wurde nur sichergestellt, dass der Strahl zur Apertur 1 kommt).
  Ist der Strahl nicht in der optischen Achse, so ändert sich nicht nur die Form im oszilloskopischen Bild, sondern der Peak beginnt auch bei Veränderung der Lens Source zu wandern.
- Scope Ap1 betätigen und Oszilloskop-Scan in X-Richtung beobachten

- Nun Lens Source erhöhen bis der Peak von einer Rechtecksform (Crossover condition in Apertur 1) in eine Dreiecksform (kein Crossover) übergeht
- Wenn der Peak zu wandern beginnt folgende Schritte durchführen:
    - Lens Source wieder auf Anfangswert zurücksetzen
    - Oszilloskop-Width auf 40 – 50 % setzen
    - Nun Justageschrauben in X-Richtung des mechanischen Alignments so drehen, dass der Peak sich in die gleiche Richtung bewegt, wie bei der Erhöhung der Lens Source
    - Den Peak für X- und Y-Achse wieder zentrieren
    - Nun Lens Source wieder erhöhen
    - Bleibt der Peak stabil oder beginnt er wieder zu wandern?
        - Wenn **Ja:** Dann ist X-Achse ausgerichtet.
        - Wenn **NEIN**: Bisherige Schritte mit "○ " wiederholen
- Ist der Strahl in X-Achse ausgerichtet, alle bisherigen Schritte für die Y-Achse wiederholen
- Die Ausrichtung ist optimal, wenn - nachdem Zentrieren des Rechtecksignals - die Spitze des Dreiecksignals sich exakt in der Mitte befindet beim Verstellen der Lens Source-Spannung.
- sich bei Drehen an Lens Source.
- Der Strom auf der Apertur 1 sollte bei einem neuen Emitter nun einen optimalen Wert von 20 bis 21 nA haben.

9. Aufnahme des regulären Messbetriebs

- Nach Schritt 8 ist die mechanische Ausrichtung des neuen Emitters abgeschlossen.
- In Übereinkunft mit Ion-TOF ist es nun zielführend die alten Setting-Files der einzelnen Betriebsmodi zu laden und die Parameter (wie bei einem normalen Start) zu optimieren.
- Darüber hinaus ist eine neue Einstellung der Massenfilter nicht zwingend erforderlich. Diese kann optional oder bei sichtbaren Problemen (z.B. ungewöhnliche Signalform am H-Signal) erfolgen.

Die folgenden Bilder sollen bei den Service-Arbeiten als Illustration dienen:

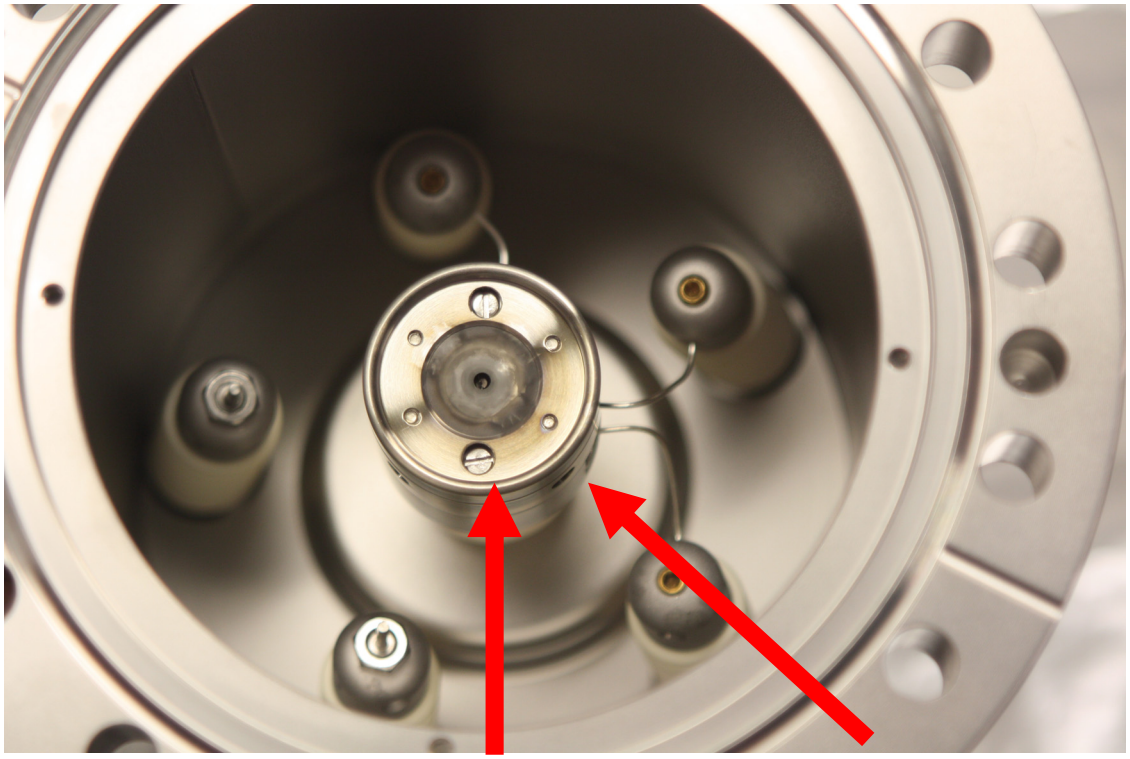

LMIG-Kopf besteht aus Emitter-Zylinder und dessen Halterung

Emitterzylinder (mit eingesetzten Emitter)

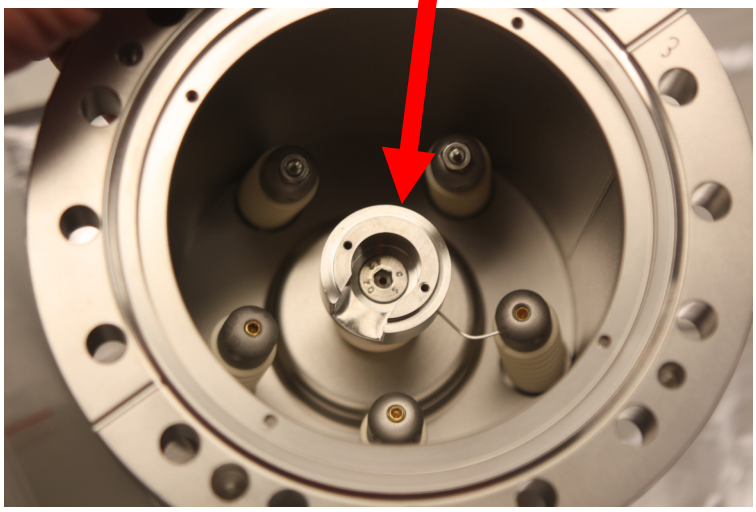

Halterung für Emitter

Aufnahme des neuen Emitters mit Emitter-Wechsel-Tool

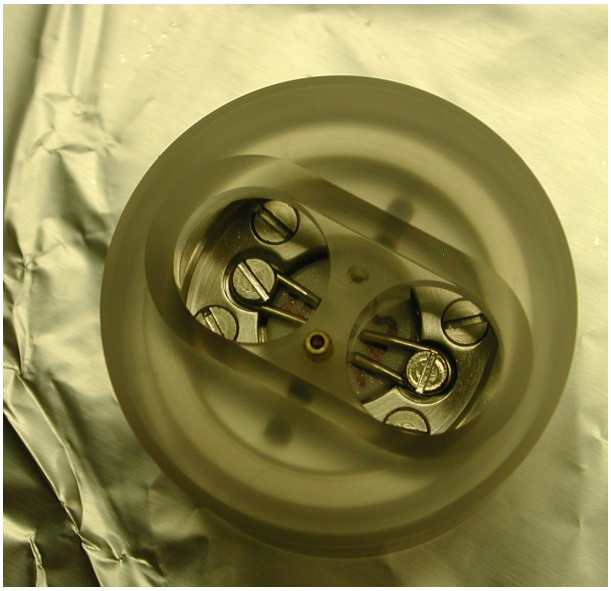

Emitter in Emitterzylinder eingesetzt
(Emitter-Wechsel-Tool noch nicht abgenommen)

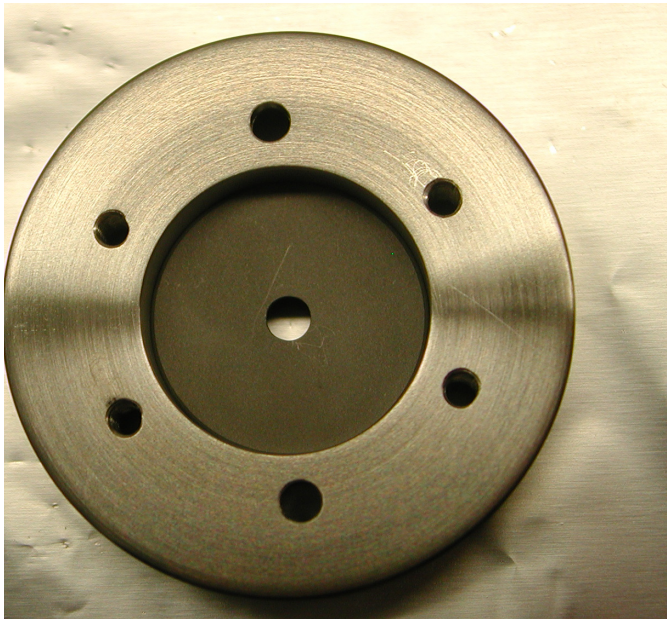

Suppressor-Apertur in Halterung eingesetzt
(im Unterteil des Emitter-Zylinders enthalten)

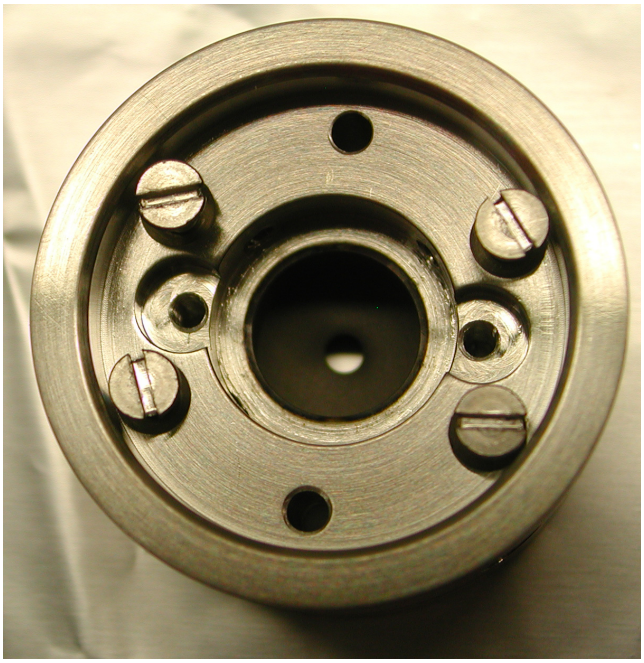

Blick von oben in den Emitter-Zylinder
(Emitter und Klemmen abgenommen)

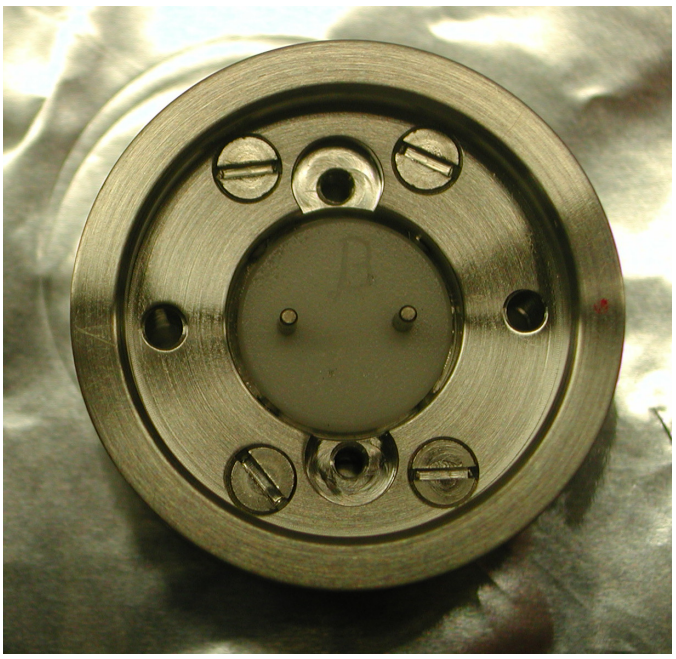

Blick von oben in den Emitter-Zylinder
(Emitter eingesetzt, aber Klemmen nicht montiert)

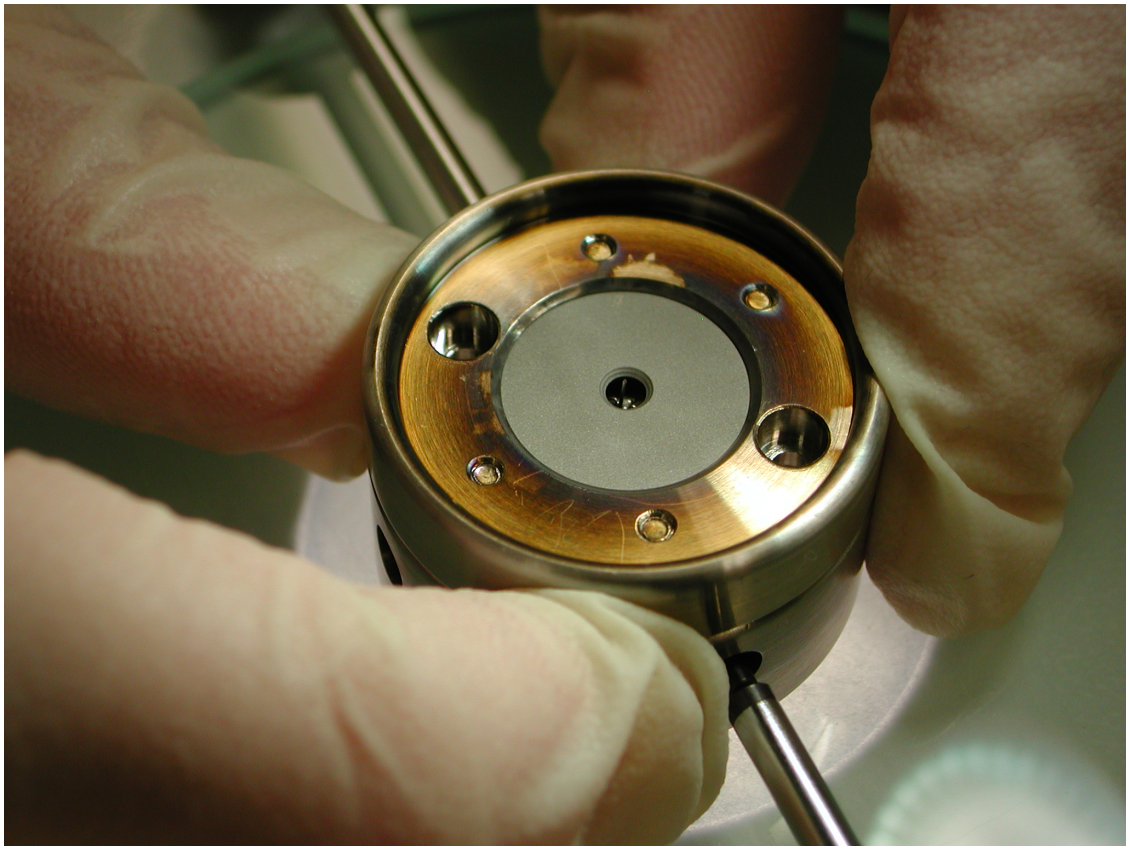

Zentrieren des Emitters (sollte unter dem Mikroskop gemacht werden)

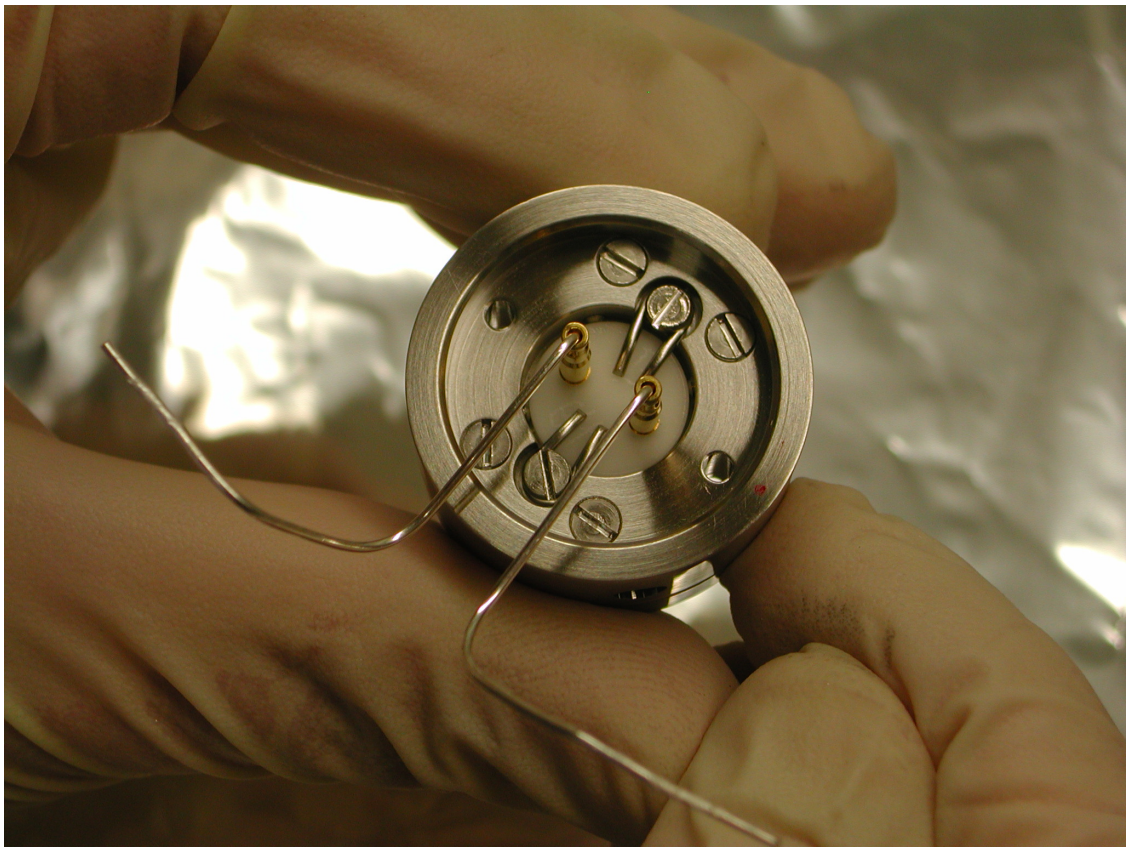

Emitter fertig zusammengebaut
(vor dem Einsetzen in den LMIG-Kopf)

Bibliography

[1] D Willoughby, DMF Cooper. Live-cell imaging cAMP dynamics. *Nature Methods*, 5(1): 29 – 36, 2008

[2] F Benabdellah, A Seyer, L Quinton, D Touboul, A Brunelle, O Laprévote. Mass spectrometry imaging of rat brain sections: nanomolar sensitivity with MALDI versus nanometer resolution by TOF–SIMS. *Analytical and Bioanalytical Chemistry*, 396(1): 151 – 162, 2010

[3] CW Freudiger, W Min, BG Saar, S Lu, GR Holtom, C H, JC Tsai, JX Kang, XS Xie. Label-Free Biomedical Imaging with High Sensitivity by Stimulated Raman Scattering Microscopy. *Science*, 322(5909): 1857 – 1861, 2008

[4] JM Berg, JL Tymoczko, L Stryer. Biochemie. *Spektrum Verlag*, Berlin, 349 – 377, 2003

[5] A Jana, EL Hogan, K Pahan. Ceramide and neurodegeneration: Susceptibility of neurons and oligodendrocytes to cell damage and death. *Journal of the Neurological Sciences*, 278(1–2): 5 – 15, 2009

[6] P Bougnoux, N Hajjaji, C Couet. The lipidome as a composite biomarker of the modifiable part of the risk of breast cancer. *Prostaglandins, Leukotrienes and Essential Fatty Acids*, 79(3-5): 93 – 96, 2008

[7] WL Holland, SA. Summers. Sphingolipids, Insulin Resistance, and Metabolic Disease: New Insights from in Vivo Manipulation of Sphingolipid Metabolism. *Endocrine Reviews*, 29(4):381 – 402, 2008

[8] R Castaing, G Slodzian. Microanalysis by secondary ionic emission. *Journal of Microscopie*, 1(6): 395 – 410, 1962

[9] A Benninghoven, E Loebach. Tandem Mass Spectrometry for Secondary Ion Studies. *Review of Scientific Instruments*, 42(1): 49 - 52, 1971

[10] RFK Herzog, F Vieböck. Ion Source for Mass Spectrography. *Physical Review*, 76(6): 855 – 856, 1949

[11] G Nagy, LD Gelb, AV Walker. An Investigation of Enhanced Secondary Ion Emission Under Au_n^+ (n = 1–7) Bombardment. *Journal of the American Society for Mass Spectrometry*, 16(5):733 – 742, 2005

[12] G Nagy, AV Walker. Enhanced secondary ion emission with a bismuth cluster ion source. *International Journal of Mass Spectrometry*, 262 (1-2): 144–153, 2007

[13] CJ Straif, H Hutter. Investigation of polymer thin films by use of Bi-cluster-ion-supported time of flight secondary ion mass spectrometry. *Analytical and Bioanalytical Chemistry*, 393(8): 1889 – 1898, 2009

[14] M Karas, D Bachmann, U Bahr, F Hillenkamp. Matrix-assisted ultraviolet laser desorption of non-volatile compounds. International *Journal of Mass Spectrometry and Ion Processes*, 78: 53 – 68, 1987

[15] F Hillenkamp, J Peter-Katalinic. MALDI MS a practical guide to instrumentation, methods and applications. *Wiley-VCH Verlag*, Weinheim, 2007

[16] C Cheng, ML Gross, E Pittenauer. Complete Structural Elucidation of Triacylglycerols by Tandem Sector Mass Spectrometry. *Analytical Chemistry*, 70(20): 4417 – 4426, 1998

[17] G Sun, K Yang, Z Zhao, S Guan, X Han, RW Gross. Matrix-Assisted Laser Desorption/Ionization Time-of-Flight Mass Spectrometric Analysis of Cellular Glycerophospholipids Enabled by Multiplexed Solvent Dependent Analyte-Matrix Interactions, *Analytical Chemistry*, 80(19): 7576 – 7585, 2008

[18] K Börner, P Malmberg, JE Mansson, H Nygren. Molecular imaging of lipids in cells and tissues. *International Journal of Mass Spectrometry,* 260(2-3): 128–136, 2007

[19] C Heim, P Sjövall, J Lausmaa, T Leefmann, V Thiel. Spectral characterisation of eight glycerolipids and their detection in natural samples using time-of-flight secondary ion mass spectrometry. *Rapid Communications in Mass Spectrometry*, 23(17): 2741 – 2753, 2009

[20] Z Cuia, M Houweling. Phosphatidylcholine and cell death. *Biochimica et Biophysica Acta*, *Molecular and Cell Biology of Lipids*, 1585(2-3): 87 - 96, 2002

[21] W Fiers, R Beyaert, W Declercq, P Vandenabeele. More than one way to die: apoptosis, necrosis and reactive oxygen damage. *Oncogene*, 18(54): 7719– 7730, 1999

[22] S Nicotera, M Leist, E Ferrando-May. Apoptosis and necrosis: different execution of the same death. *Biochemical Society Symposia*, 66: 69 - 73, 1999

[23] JJ Lemasters. Necrapoptosis and the mitochondrial permeability transition: shared pathways to necrosis and apoptosis. *American Journal of Physiology*, *Gastrointestinal and Liver Physiology*, 276(1): 1 – 6, 1999

[24] Helpfile of the ToF-SIMS^5 instrument, Version 5.0, Ion TOF GmbH, Germany